Saudi Journal of Biological Sciences 27 (2020) 1538–1552

Contents lists available at ScienceDirect

Saudi Journal of Biological Sciences

journal homepage: www.sciencedirect.com

Original article

Curcumin-loaded cockle shell-derived calcium carbonate nanoparticles: A novel strategy for the treatment of lead-induced hepato-renal toxicity in rats

Maryam Muhammad Mailafiya [a,b], Kabeer Abubakar [a,b], Samaila Musa Chiroma [c], Abubakar Danmaigoro [d], Ezamin Bin Abdul Rahim [e], Mohamad Aris Mohd Moklas [a,*], Zuki Abu Bakar Zakaria [f]

[a] Department of Human Anatomy, Faculty of Medicine and Health Sciences, University Putra Malaysia, 43400 Serdang, Selangor Darul Ehsan, Malaysia
[b] Department of Human Anatomy, College of Medical Sciences, Federal University Lafia, 950101, Akunza, Lafia, Nasarawa State, Nigeria
[c] Department of Human Anatomy, Faculty of Basic Medical Sciences, University of Maiduguri, 600230 Maiduguri, Borno State, Nigeria
[d] Department of Veterinary Anatomy, Faculty of Veterinary Medicine, Usman Danfodiyo University, 840213, Sultan Abubakar, Sokoto State, Nigeria
[e] Department of Radiology, Faculty of Medicine and Health Sciences, University Putra Malaysia, Serdang 43400, Selangor Darul Ehsan, Malaysia
[f] Department of Preclinical Sciences Faculty of Veterinary Medicine, University Putra Malaysia, Serdang 43400, Selangor Darul Ehsan, Malaysia

ARTICLE INFO

Article history:
Received 7 November 2019
Revised 4 March 2020
Accepted 4 March 2020
Available online 12 March 2020

Keywords:
Hepato-renal injuries
Lead-toxicity
Cockle shell
Curcumin
Nanoparticles
Oral therapeutics

ABSTRACT

Lead (Pb) toxicity affects the hepatic and renal systems resulting to homeostasis imbalance. Curcumin is a strong antioxidant but has restrained clinical applications due to its poor bioavailability. Nanomedicine showed promising potentials in drug delivery and has brought forth the use of cockle shell-derived aragonite calcium carbonate nanoparticles ($CSCaCO_3NP$) to enhance the effectiveness and targeted delivery of curcumin (Cur). Thus, this study aimed at evaluating the therapeutic effect of curcumin-loaded $CSCaCO_3NP$ (Cur- $CSCaCO_3NP$) on lead-induced hepato-renal toxicity in rats. Thirty-six male adults Sprague-Dawley rats were randomly assigned into five groups. All groups contained six rats each except for group A, which contained 12 rats. All rats apart from the rats in group A (control) were orally administered a flat dose of 50 mg/kg of lead for four weeks. Six rats from group A and B were euthanized after four weeks of lead induction. Oral administration of curcumin (100 mg/kg) for group C and Cur-$CSCaCO_3NP$ (50 and 100 mg/kg) for groups D and E respectively, commenced immediately after 4 weeks of lead induction which lasted for 4 weeks. All rats were euthanized at the 8th week of the experiment. Further, biochemical, histological and hematological analysis were performed. The findings revealed a biochemical, hematological and histological changes in lead-induced rats. However, treatments with the Cur-$CSCaCO_3NP$ and free curcumin reversed the aforementioned changes. Although, Cur-$CSCaCO_3NP$ presented better therapeutic effects on lead-induced toxicity in rats when compared to free curcumin as there was significant improvements in hematological, biochemical and histological changes which is parallel with attenuation of oxidative stress. The findings of the current study hold great prospects for Cur-$CSCaCO_3NP$ as a novel approach for effective oral treatment of lead-induced hepato-renal impairments.

1. Introduction

Lead (Pb) is one of the oldest ubiquitous naturally occurring toxic metal with rapid increase of contamination and intoxication to various biological systems leading to serious deleterious effects (Haleagrahara et al., 2011; Jarvis et al., 2018). Lead toxicity remained a significant global burden with multiple physiological problem associated with renal and hepatic dysfunction (Mason et al., 2014; Vorvolakos et al., 2016). Despite the well-known health-related hazards of lead, its industrial usage is still considered due to its favourable physicochemical properties resulting

* Corresponding author at: Department of Human Anatomy, Faculty of Medicine and Health Sciences, University Putra Malaysia, 43400 Serdang, Selangor Darul Ehsan, Malaysia.
E-mail address: aris@upm.edu.my (M.A. Mohd Moklas).

Peer review under responsibility of King Saud University.

Production and hosting by Elsevier

https://doi.org/10.1016/j.sjbs.2020.03.009
1319-562X/

to high environmental accumulation as such resulting to prone contamination by the inhabitants (Wani et al., 2015; Jarvis et al., 2018). According to institute for health and metrics evaluation IHME, (IHME, 2017), lead toxicity accounted for about 494,550 deaths and 9.3 million disability-adjusted life years (DALYs) due to long-term effects on health based on WHO (2015) data estimates (WHO, 2015). Further, Jacobs et al. (2002), reported that about 24 million people of the US population had significant lead hazards of which, 1.2 million are low-income families (< $30,000/year). It is worthy to know that one of the common mechanisms of lead toxicity is via oxidative stress which consequently results to serious health pathological conditions (Vlasak et al., 2019).

Studies have shown that sub-chronic oral administration of different doses of lead revealed blood, liver and kidney to be the main target organs (Yuan et al., 2014; Andjelkovic et al., 2019). The liver and kidney are highly vulnerable to lead upon exposure at both low and high levels that could result to acute or chronic liver and kidney dysfunctions (Andjelkovic et al., 2019; Kabeer et al., 2019). Therefore, exposure to lead may lead to significant alterations of the activities of these functional enzymes (Alwaleedi, 2016). In addition, usual occurrences of hepato-renal toxicity due to lead exposure is primarily attributed to oxidative stress (Flora et al., 2012). Consequently, the scientific search for effective and nontoxic natural compounds with potential antioxidant activities has been a call of concern (García-Niño and Pedraza-Chaverrí, 2014). Thus, natural antioxidant such as curcumin have been reported to possess the ability of both preventing and curing the various lead-induced pathological conditions by quenching the excessive free radicals generated (Flora et al., 2012).

Recently the use of phytochemicals in pharmaceutical drug industry is attracting attentions particularly with regard to the use of a natural compound such as curcumin as a proposed alternative and effective strategy in the treatment of heavy metal induced toxicity (Hae et al., 2007; Abu-taweel, 2018). Curcumin possesses an outstanding safety profile with various documented therapeutic activities including antioxidant and anti-inflammatory properties (Agarwal et al., 2010). To date, pharmacokinetic studies emphasizes on the major setbacks behind curcumin poor bioavailability to be; poor aqueous solubility and rapid clearance due to fast metabolism at the GIT (Chirio et al., 2019; Yavarpour-bali et al., 2019). Robust strategies in nanotechnology have been pursued to enhance the oral bioavailability of curcumin thereby boosting its therapeutic efficacy (Li et al., 2019). Moreover, many delivery systems are synthesized from inorganic sources or assembled polymers for curcumin delivery, however, they are associated with multiple nano-toxic effects which could jeopardize the quality effect of the nanoparticles (Giner-Casares et al., 2016). This has necessitated the search for natural inorganic material such as $CSCaCO_3NP$ for curcumin delivery to boost the therapeutic efficacy of curcumin.

Cockle shells are natural shells of marine bivalve molluscs which are excellent sources of calcium carbonate normally used as nanocarriers in drug delivery (Mailafiya et al., 2019). Impressive studies on targeted drug delivery system have shown the useful usage of $CSCaCO_3NP$ for the treatment of many ailments using different drugs which presented encouraging impressive results (Kamba et al., 2013; Danmaigoro et al., 2017; Hammadi et al., 2017; Hamidu et al., 2019). Noteworthy, based on previous studies, the application of this nanocarrier was limited to only standard drugs via intravenous administration for the treatment of cancerous diseases. Thus, therapeutic effect of curcumin-loaded cockle shell derived calcium carbonate (aragonite) nanoparticles on lead-induced hepato-renal toxicity in rats has not been studied.

In addition, apart from the documented reports on the use of $CSCaCO_3NP$ as a bone-remodelling agent and for the delivery of anticancer and anti-bacterial drugs (Kamba et al., 2013; Isa et al., 2016; Danmaigoro et al., 2017; Fu et al., 2017), the current research becomes an added advantage on the multiple applications of $CSCaCO_3NP$ for the delivery of antioxidant therapeutics. It is solely believed that the current findings will provide a valuable confirmation of the therapeutic effect of Cur-$CSCaCO_3NP$ on liver and kidney diseases. Noteworthy, previous study documented that both $CSCaCO_3NP$ and Cur-$CSCaCO_3NP$ to be nontoxic to normal cells *in vitro* (Mailafiya et al., 2019). Hence, this research stressed on not only targeted effect mechanism of $CSCaCO_3NP$ but also the ability of the nanoparticle to improve the efficacy of curcumin primarily via enhanced attenuation of oxidative stress. Hence, the research aimed at evaluating the therapeutic effect of curcumin-loaded cockle shell-derived calcium carbonate nanoparticles on lead-induced hepato-renal toxicity in rats by the assessments of oxidative stress biomarkers, liver and kidney function tests, hematological and histological assessments.

2. Materials and methods

2.1. Chemical, reagents and kits

Cockle shell was purchased from Malaysian local wet market. Lead acetate (99%) and rat feed were obtained from Sigma-Aldrich (St. Louis, MO, USA). Fixatives, H and E stain were purchased from Sigma Aldrich St. Louis Co., United State. Toluidine Blue stain was obtained from Agar scientific (Agar scientific Ltd, UK). In addition, normal saline was obtained from Apical Scientific Sdn, Bhd Malaysia. Kits includes; Superoxide Dismutase (SOD) assay kit (E-BC-K020, Elabscience biotechnology Inc.), Elisa kit (Elabscience biotechnology Inc.) and Pierce™ BCA protein assay kit (Thermo Fisher Scientific, Carlsbad, CA, USA). All other reagents, kits and chemicals used were of higher purity.

2.2. Animals

Healthy thirty-six (36) adult male Sprague-Dawley rats (8 weeks old) with the average body weight ranging between 200 and 250 g were used in this study. The rats were obtained from the Animal Breeding Unit, Faculty of Veterinary Medicine, Universiti Putra Malaysia. The rats were kept in plastic cages and maintained at the same laboratory conditions (temperature of 25 °C ± 2 °C, 12 h light: 12 dark cycle) for one week of acclimatization at the Faculty of Medicine and Health Sciences, Universiti Putra Malaysia. All rats had free access to food and water a*d libitum* throughout the study period. The animal management and care procedures were performed in accordance to the standard procedure of the organization for economic co-operation and development (OECD) recommended guidelines. Further, the experiment was approved by the Institutional Animal Care Committee (IACUC) of the Universiti Putra Malaysia (UPM/IACUC/AUP-R038/2018).

2.3. Synthesis of $CSCaCO_3NP$ and Cur-$CSCaCO_3NP$

The preparation, synthesis, loading processes and physicochemical characterizations of $CSCaCO_3NP$ and Cur-$CSCaCO_3NP$ were described in the previous work of Mailafiya et al. (2019). Noteworthy, based on the protocol and the loading procedure of the author's previous study, the best formulation of Cur-$CSCaCO_3NP$ that presented the most suitable loading content and encapsulation efficiency was selected for curcumin delivery.

2.4. Experimental design

The rats were randomly assigned into five groups (A, B, C, D and E) after acclimatization, which comprises of the control (normal

saline and water), lead treated group (LTG) and three treatment groups (lead and free curcumin, lead and Cur-CSCaCO$_3$NP).. The experimental design consists of two phases, which are the induction phase, and the treatment phase. The induction phase involved the oral administration of lead at a flat dose of 50 mg/kg for four weeks (three times a week) to all the rat's groups except the control group (Table 1). The method of lead induction for this experiment follows the standard procedures of Owolabi, (2012) and Ayuba et al. (2017) and the overall experimental administration method was in accordance to the work of Sankar et al. (2013) with slight modifications. At the end of the first phase of the experiment, six rats from the control group and the whole of group B were euthanized to confirm the lead toxic effects. The second phase of the experiment commenced with the oral treatment with free curcumin (100 mg/kg three times a week for group C) and Cur-CSCaCO$_3$NP (50 mg/kg and 100 mg/kg three times a week for groups D and E respectively) for four weeks (three times a week) as shown in Table 1. The induction phase and treatment phase lasted for four weeks each and the overall experiment lasted for 8 weeks.

2.5. Dose preparation and determination of lead and Cur-CSCaCO$_3$NP

Lead acetate solution was prepared by dissolving 1 g of lead in 50 ml of deionized water to form a stock solution of 20 mg/ml of lead acetate concentration. A dose of 50 mg/kg was given to each rat base on the body weight (Sidhu and Nehru, 2004; Owolabi, 2012; Ayuba et al., 2017). The choice of oral administration of lead at a dose of 50 mg/kg in this study was adopted to demonstrate environmental mimicked lead exposure. The common direct culprit of environmental lead exposure is mostly via ingestion particularly in drinking water (Bhattacharjee et al., 2018). In addition, lead exposure resulted to several pathological conditions on the populations exposed to it even at low level (Flora et al., 2012; Husain, 2015). Thus, regardless of the higher amount of lead exposure, cumulative dose of lead and vulnerability of the individual are strongly linked to health consequences (Kim et al., 2014; Bose-O'Reilly et al., 2017). The Cur-CSCaCO$_3$NP was weighed to get the exact amount of dose needed for the rats (i.e. 100 mg/kg and 50 mg/kg) from which a stock solution was made by dissolving in 50 ml of deionized water. Each rat was given a dose of 50 mg/kg (group D) and 50 mg/kg (group E) base on the body weight. The dose of free curcumin at 100 mg/kg was reported to be nontoxic in rats, in fact higher dose of curcumin showed no evidence of toxicity indicating its wide safety level (Sarada et al., 2015; Zhang et al., 2018). Further, studies have shown that CSCaCO$_3$NP possess wide safety margin to biological system (Jaji et al., 2017; Danmaigoro et al., 2018; Mailafiya et al., 2019). In addition, documented *in vitro* studies reported the safety and biocompatibility effect of CSCaCO$_3$NP on various cell lines (Kamba et al., 2014; Fu et al., 2017; Hamidu et al., 2019; Mailafiya et al., 2019).

2.6. Blood sample collection

Prior to euthanasia, at 8th week all the rats were anesthetized with xylazine (100 mg/kg) + ketamine (100 mg/kg) by intramuscu-

Table 1
Experimental design for four weeks of lead induction and four weeks of curcumin and Cur-CSCaCO$_3$NP treatment in rats.

Groups	Description	Induction phase	Number of rats	Euthanasia
A	Control	Normal saline	12	6 rats
B	LTG	Pb (50 mg/kg)	6	6 rats
C	Experimental 1	Pb (50 mg/kg)	6	-
D	Experimental 2	Pb (50 mg/kg)	6	-
E	Experimental 3	Pb (50 mg/kg)	6	-
Weeks	1 → 4			
Groups	**Description**	**Treatment phase**	**Number of rats**	**Euthanasia**
A	Control	Normal saline	6	6 rats
B	LTG	-	-	-
C	Cur 100	Curcumin (100 mg/kg)	6	6 rats
D	Cur-CSCaCO$_3$NP 50	Cur-CSCaCO$_3$NP (50 mg/kg)	6	6 rats
E	Cur-CSCaCO$_3$NP 100	Cur-CSCaCO$_3$NP (100 mg/kg)	6	6 rats
Weeks	5 → 8			

Note: lead treated groups (LTG), curcumin 100 mg/kg (Cur 100), curcumin-loaded cockle shell-derived calcium carbonate nanoparticles (Cur-CSCaCO$_3$NP 50 and 100) and Lead (Pb).

lar injection. The blood sample was collected via cardiac puncture through the diaphragm for the following hematological examinations; one aliquot of blood with anticoagulant (heparin) was used for the measurement of complete blood counts (Hemogram) and second aliquot with anticoagulant (heparinized EDTA) was used to obtain plasma. The remaining amount of blood was collected in non-heparinized test tube (plain tube) for obtaining serum. Serum and plasma were separated by whole blood centrifugation at 4000 rpm for 15 min using centrifuge Eppendorf 5424R, Germany, and stored in (-80 °C for plasma and −20 °C for serum) for biochemical assays and assessment of oxidative stress biomarkers respectively. Organs of interest such as; kidney and liver were harvested, washed thrice in ice-cold saline and weighed then stored in 10% formalin for histological and histochemical analysis.

2.7. Hematology and biochemical analysis

Blood samples collected were immediately analyzed for complete blood count using Horiba Medical Scil Vet ABC Plus analyzer (Scil Vet, USA). The following hematological parameters were assessed; Red blood cells (RBC), platelets (PLT), hemoglobin (Hb), packed cell volumes (PCV), mean corpuscular volume (MCV), mean corpuscular hemoglobin (MCH), mean corpuscular hemoglobin concentration (MCHC), white blood cells (WBC), monocytes, neutrophils, eosinophil and lymphocytes. The kidney and liver function enzymes were analyzed with commercial reagents and according to good laboratory practice on the Dimension Xpand Plus Integrated Chemistry System analyzer (Dimension EXL, 200 integrated Chemistry System, Siemens, Germany) for the following parameters: creatinine, urea, total protein (TP), albumin (ALB), total bilirubin (Tbil), globulin, gamma-glutamyl transferase (GGT), lactate dehydrogenase (LDH), alkaline phosphatase (ALP), aspartate aminotransferase (AST) and alanine aminotransferase (ALT)

2.8. Redox status analysis

Serum SOD activities and MDA levels were quantified using colorimetric methods base on their respective assay kits.

2.8.1. Enzyme linked-immunosorbent assay (ELISA)

Malondialdehyde (MDA) level was quantified from the rats' serum strictly base on the simple principle of competitive-ELISA using MDA ELISA kit (E-EL-006, Elabscience). MDA level was assayed by monitoring the competitive reaction of the fixed amount of MDA on the pre-coated microtitter plate surface with the MDA in the serum samples. Standard working solution was set up for each sample well and 50 μL of the sample were added in each well separately. Immediately, biotinylated detection Ab working solution was added to each well sealed and incubated for 45 min at 37 °C. The solutions were aspirated and 350 μL of buffer was added to each well and soaked for 2 min then aspirated again 3 times before the addition of 100 μL of HRP conjugate working solution to each well and incubated for 30 min at 37 °C. Further, the incubated solution was decanted and washed with buffer solution 5 times before the addition of 90 μL of substrate reagent to each well and incubated for 15 min at 37 °C. Finally, 50 μL of stop solution was added to each well and the absorbance was measured using a micro-plate reader at a wavelength of 450 nm. The results were expressed as ng/mL.

2.8.2. Superoxide dismutase (SOD) activity analysis

Assessments of the SOD activities in the rats' serum using the method of colorimetric analysis of WST-1 product was strictly base on the kit's instructions. The reaction mixture comprises of the following; 20 μL of tissue homogenates, 20 μL of enzyme working solution and 200 μL of substrate application solution. These solutions were fully mixed and incubated at 37 °C for 20 min. The final absorbance was taken at a wavelength of 450 nm and the results were expressed in U/mL.

2.9. Histopathological analysis

The fixed liver and kidney tissues were processed for histological evaluation as described in the previous study Danmaigoro et al. (2018). The tissues were trimmed, inserted in plastic cassettes and dehydrated in ascending degree of alcohol solutions and absolute alcohol, cleared in xylene and infiltrated in liquid paraffin and finally embedded in paraffin wax using an automated tissue processor (Leica TP 1020, Semi enclosed benchtop tissue processor, Singapore). The tissue sectioning microtome (Leica 2235 Microtome, USA) was used to trim and sectioned to approximately 5 μm thick in size. The sectioned tissue ribbon was suspended on the surface of warm water bath, picked using clean glass slides, and allowed to dry. Finally, the sectioned liver, kidney was stained using the standard techniques for H & E for normal histology study and examined under the light microscope (Leica DM4M, NY USA). Moticam Pro 282A 5.0MP (Motic images Software Plus 2.0 TWAIN, Hong Kong) was used to analyse the degree of tissue injury, necrosis and inflammatory responses.

2.9.1. Histopathological tissue scoring system

A minimum of three sections of each tissues were taken for evaluation in five rats per group (n = 5). Toxicological lesions such as activated Kupffer cells, sign of necrosis, vaculation (Fatty changes), inflammatory cell infiltrations, karyolysis, pyknotic cells and karyorrhexis in the liver were examined and scored. Meanwhile in kidney tissue, toxicological lesions such as sign of necrosis, tubular dilatation, inflammatory cells, eosinophilic cytoplasm, atrophy of glomerulus and fatty degeneration were examined and scored. The scoring assessments were performed through a guide of two independent histologists. The overall methods of tissue scoring system was in accordance with the previous literatures (Asyura et al., 2016; Nurul et al., 2018). The detailed description of lesion scoring method for both kidney and liver are presented in Table 2.

2.10. Statistical analysis

All analysis was conducted using SPSS version 25 and GraphPad prism (GraphPad Prism software, Inc, Version 6.01, San Diego, California, USA). The differences in p values < 0.05 were statistically significant. The data obtained were presented as mean ± standard error of mean (SEM). Data obtained from the effect of lead on various parameters was conducted using student unpaired-samples t-test. Further, the data obtained from effect of free curcumin and Cur-CSCaCO$_3$NP on various parameters was analysed using one-way analysis of variance (ANOVA) followed by Tukey's post-hoc test. While the data obtained from histology was

Table 2
Lesion scoring system for kidney and liver tissues (Asyura et al., 2016; Nurul et al., 2018).

Score	Percentage	Severity
0	None	None
0.5	<15%	Very mild
1	15–30%	mild
1.5	30–45%	Mild to moderate
2	45–60%	Moderate
2.5	60–75%	Moderate-severe
3	More than 75%	Severe

conducted using non-parametric *t*-test followed by Mann Whitney *U* test for the effect of lead on various tissues and one-way ANOVA followed by Kruskal Wallis test for global comparison of organ lesions for the effect of free curcumin and Cur-CSCaCO$_3$NP. Dunn's test was used to assessed the statistical differences among the groups.

3. Results

3.1. Effects of lead on the weight of organs

There was a significant difference between the weight of all the organs of lead-induced rats and the control group of rats as demonstrated by the Unpaired-samples *t*-test as follows; Liver [LTG (11.13 ± 0.4013)g] and the control group of rats (9.448 ± 0.3580)g, $p = 0.0108$, Right kidney [LTG (3.092 ± 0.2185)g] and the control group of rats (2.313 ± 0.1716)g, $p = 0.0187$. In addition, a statistically significant difference was observed between the left kidney [LTG (2.125 ± 0.2323) g] and the control groups of rats (2.903 ± 0.09807)g $p = 0.0115$. These results showed that lead significantly increased the weights of the liver, left and right kidneys of the rats when compared to their respective controls (Fig. 1).

3.2. Effects of Cur-CSCaCO$_3$NP on the weight of organs

As shown in Fig. 2, one-way ANOVA revealed statistically significant difference in the weight of the liver of rats [F (3, 20) = 7.218, $p = 0.0018$]. Tukey's post hoc revealed significant decrease in the weight of the liver of the rats treated with Cur-CSCaCO$_3$NP 100 (8.56 ± 0.27 g, $p = 0.01$) and the control group (8.5 ± 0.38, $p = 0.0021$) when compared to Cur 100 treatment group (1.613 ± 0.064) g. No differences were observed in the weight of right and left kidney between the control, Cur 100, Cur-CSCaCO$_3$NP 50 and Cur-CSCaCO$_3$NP 100 treated groups of rats.

3.3. Effect of lead on kidney biochemical analysis and liver function test

Acute lead induction resulted in altered profile of the biochemical parameters in rats. An unpaired-samples *t*-test was conducted to compare the difference in the levels of creatinine and urea from serum of rats in the lead treated group and the control groups as shown in Fig. 3. There was a significant increase in creatinine (41.80 ± 3.20) in the lead-administered rats when compared to the control (63.20 ± 4.13), $p = 0.0035$. Similarly, a significant increase in the serum level of urea concentrations in LTG group (7.72 ± 0.34) when compared to the control group (6.66 ± 0.23),

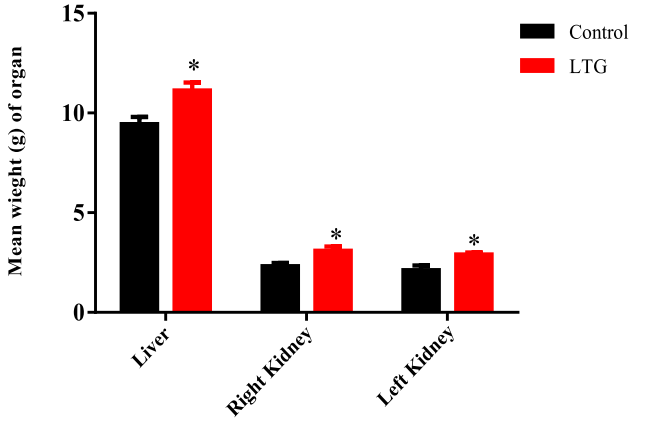

Fig. 1. Effects of lead on the weight of organs in rats after 4 weeks of induction. Values were presented as mean ± SEM, n = 6. * $p < 0.05$ vs control group.

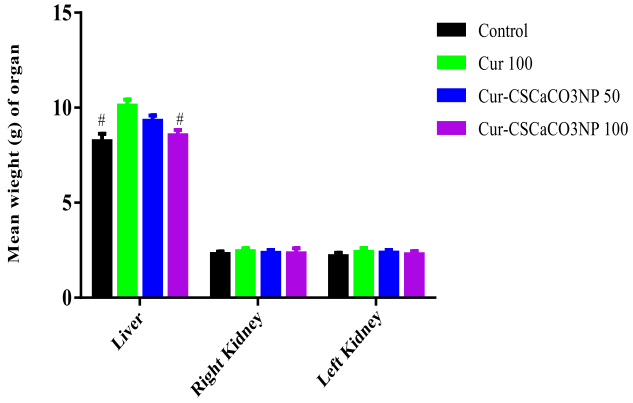

Fig. 2. Effects of Cur-CSCaCO$_3$NP and curcumin on the weight of organs in rats exposed to lead. Values were presented as mean ± SEM, n = 6. # $p < 0.05$ vs Cur 100 group.

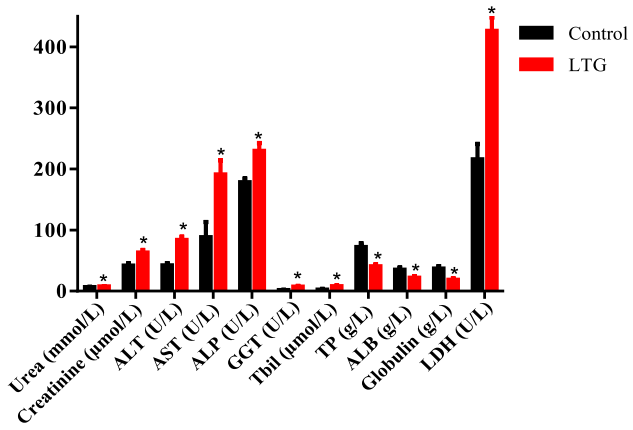

Fig. 3. Effects of lead on serum biochemical parameters in rats after acute lead-induction. Values were presented as mean ± SEM, n = 5. *$p < 0.05$ vs control.

$p = 0.03$ was observed. This result demonstrated an increase in the two parameters of kidney function caused by oral administration of lead.

Assessment of the effect of lead on liver function of the serum of lead-administered rats was conducted using unpaired-samples *t*-test as shown in Fig. 3. The difference in the mean of the following biochemical parameters revealed a significant increase as follows: ALT [LTG (83.80 ± 5.33)], when compared to the control group (42.00 ± 3.67), $p = 0.0002$, AST [LTG (88.40 ± 24.78)] when compared to the control group (191.0 ± 23.49), $p = 0.0169$, ALP [LTG (229.6 ± 12.81)] when compared to the control group (178.4 ± 5.83), $p = 0.0066$, GGT [LTG (7.160 ± 1.24)] when compared to the control group (1.69 ± 0.43), $p = 0.0031$, Tbil [LTG (2.52 ± 1.06)] when compared to the control group (8.16 ± 0.96), $p = 0.0042$ and LDH [LTG (426.2 ± 21.73)] when compared to the control group (215.8 ± 25.14), $p = 0.0002$. Conversely, a significant decrease in the following biochemical parameters were observed; globulin [LTG (18.56 ± 2.25)] when compared to the control group (37.12 ± 3.60), $p = 0.0024$, ALB [LTG (22.08 ± 2.59)] when compared to the control group (34.96 ± 3.51), $p = 0.0183$ and TP [LTG (40.64 ± 3.17)] when compared to the control group (72.08 ± 6.17) , $p = 0.0019$.

3.4. Effects of Cur-CSCaCO$_3$NP on kidney and liver biochemical analysis

One-way ANOVA employed to analyze the protective effect of Cur-CSCaCO$_3$NP and curcumin on kidney functions demonstrated significant differences in creatinine and urea levels in the rat's

serum after four weeks of treatments [Creatinine: F (3, 16) = 4.697, p = 0.0155, Urea: F (3, 16) = 5.29, p = 0.01]. Tukey's post hoc revealed significant decreases of creatinine levels in the serum of the control groups (40.18 ± 2.09, p = 0.0183) and Cur-CSCaCO$_3$NP 100 groups of rats (40.80 ± 1.20, p = 0.0308) when compared to Cur 100 groups (48.20 ± 2.18). Further, a significant decrease in the levels of urea in the serum of the control group (5.944 ± 0.255, p = 0.017) and Cur-CSCaCO$_3$NP 100 groups of rats (6.10 ± 0.36, p = 0.0421) when compared to Cur 100 groups (7.10 ± 0.16). There were no statistically significant differences in the mean of the Cur-CSCaCO$_3$NP 100 groups of rats when compared to their respective control group (Fig. 4).

As shown in Fig. 4, One-way ANOVA used to analyze the protective effect of Cur-CSCaCO$_3$NP and curcumin on liver functions showed significant differences [ALT: F (3, 16) = 6.836, p = 0.0035, GGT: F (3, 16) = 10.81, p = 0.0004, Tbil: F (3, 16) = 4.232, p = 0.0221, LDH: F (3, 16) = 6.066, p = 0.0059 and TP: F (3, 16) = 6.209, p = 0.0053]. Tukey's post hoc revealed significant decrease in ALT levels in the serum of the control group (40.20 ± 4.20, p = 0.0032), Cur-CSCaCO$_3$NP 50 group (48.80 ± 2.91, p = 0.0417) and Cur-CSCaCO$_3$NP 100 group of rats (45.40 ± 6.43, p = 0.0154) when compared to Cur 100 group (68.80 ± 4.91). A significant decrease in the levels of AST in the serum of the control group (1.87 ± 0.04, p = 0.0005), Cur-CSCaCO$_3$NP 50 group (3.12 ± 0.22, p = 0.0458) and Cur-CSCaCO$_3$NP 100 group of rats (2.17 ± 0.18, p = 0.0014) when compared to Cur 100 groups (4.75 ± 0.74). Also, significant decrease in the levels of serum Tbil of the control group (1.74 ± 0.07, p = 0.0265) and Cur-CSCaCO$_3$NP 100 group of rats (1.97 ± 0.25, p = 0.0466) when compared to Cur 100 group (4.26 ± 1.08). Further, a significant decrease was observed in the mean LDH of the control group (207.2 ± 14.86, p = 0.0093), Cur-CSCaCO$_3$NP 50 (225.6 ± 32.08, p = 0.0209) and Cur-CSCaCO$_3$NP 100 (222.2 ± 28.32, p = 0.0180) when compared to the Cur 100 group of rats (376.6 ± 46.04). Conversely, a significant increase in TP was observed in the control group (74.64 ± 3.34, p = 0.0049) and Cur-CSCaCO$_3$NP 100 groups of rats (70.92 ± 2.14, p = 0.0184) when compared to the Cur 100 group of rats (51.66 ± 3.29, p =). No statistically significant differences were observed in the levels of AST, ALP, ALB and globulin among all the treatment groups when compared to their respective control groups of rats.

3.5. Effect of lead on leukogram in rats

Unpaired independent t-test was used to evaluate the effect of lead on leukogram in rats. The results showed a significant elevation of all the leukogram parameters of lead-induced rats when compared to their respective control groups of rats as follows: White blood cells (WBC) [LTG (16.34 ± 0.62)] when compared to the control group (6.10 ± 0.61), p < 0.0001, neutrophils [LTG (3.02 ± 0.06)] when compared to the control group (1.10 ± 0.26), p < 0.0001, lymphocytes [LTG (8.46 ± 0.23)] when compared to the control group (5.29 ± 1.09), p = 0.0217, monocytes [LTG (0.35 ± 0.06)] when compared to the control group (0.09 ± 0.01), p = 0.0016 and eosinophils [LTG (0.27 ± 0.06)] when compared to the control group (0.084 ± 0.0051), p = 0.0134 (Fig. 5).

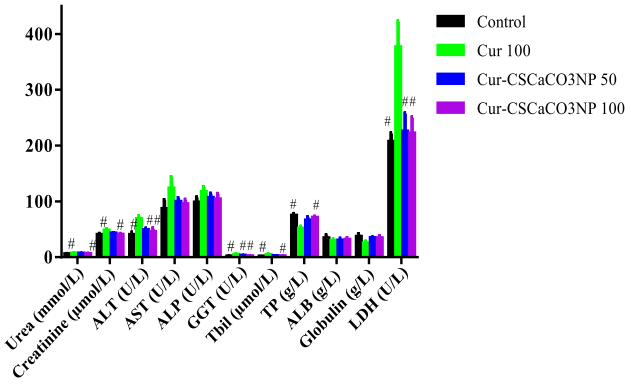

Fig. 4. Effects of Cur-CSCaCO$_3$NP and curcumin on serum biochemical parameters of lead-administered rats. Values were presented as mean ± SEM, n = 5. # P < 0.05 vs Cur 100.

3.6. Effect of Cur-CSCaCO$_3$NP on leukogram

One-way ANOVA was used to analyze the mean differences in the leukogram parameters of the control group and lead treated group of rats. Statistically significant differences were observed in the neutrophil's levels: [F (3, 16) = 4.243, p = 0.0219]. Tukey's post hoc revealed statistically significant decrease in the neutrophils level of rats in the control group (1.11 ± 0.13) and Cur-CSCaCO$_3$NP 100 groups of rats (1.19 ± 0.25), when compared to the Cur 100 (2.09 ± 0.092) groups of rats. No statistically significant difference was observed in the level of neutrophils in the Cur-CSCaCO$_3$NP 50 group when compared to the control groups of rats. Further, no significant differences in the levels of WBC, lymphocytes, monocytes, eosinophils among the mean of rats in all the treatment groups when compared to their control groups of rats as shown in Fig. 6.

3.7. Effect of lead on hematological indices in rats

An independent t-test was used to analyze the mean differences in the hematological parameters of the control group and lead treated group of rats (Fig. 7). The results showed statistical significant decrease in the mean of the lead treated group when compared to their control groups of rats as follows: Red blood cells (RBC) [LTG (5.76 ± 0.38)] when compared to the control group (9.002 ± 0.32), p = 0.0002, hemoglobin (Hb) [LTG (6.61 ± 0.35)] when compared to the control group (10.66 ± 0.14), p < 0.0001, PCV [LTG (32.20 ± 1.74)] when compared to the control group (49.80 ± 1.53), p < 0.0001, MCV [LTG (50.56 ± 1.11)] when compared to the control group (55.41 ± 1.17), p = 0.0165, MCH [LTG (9.86 ± 0.52)] when compared to the control group (14.05 ± 0.22), p < 0.0001 and MCHC [LTG (33.86 ± 1.86)] when compared to the control group (19.15 ± 0.51), p < 0.0001. Further, a significant increase in the volume of platelets (PLT) [LTG (984.4 ± 94.38)] when compared to the control group (520.8 ± 171.0), p = 0.0450.

3.8. Effects of Cur-CSCaCO$_3$NP on hemogram of lead-induced rats

To investigate the therapeutic effect of Cur-CSCaCO$_3$NP and curcumin on lead-administered rats, the volume of hematological

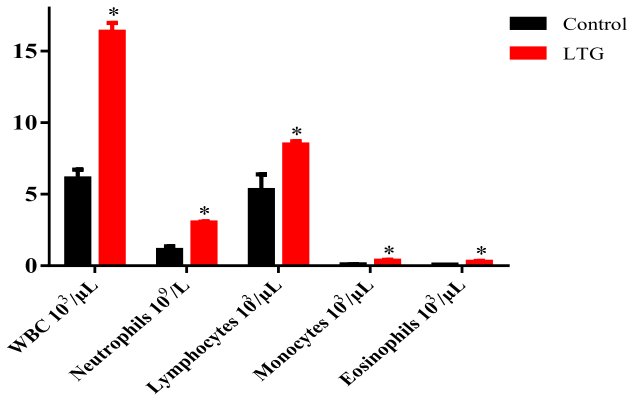

Fig. 5. Effect of lead on leukogram in rat's blood after induction. Values were presented as mean ± SEM, n = 5, *p < 0.05 vs control.

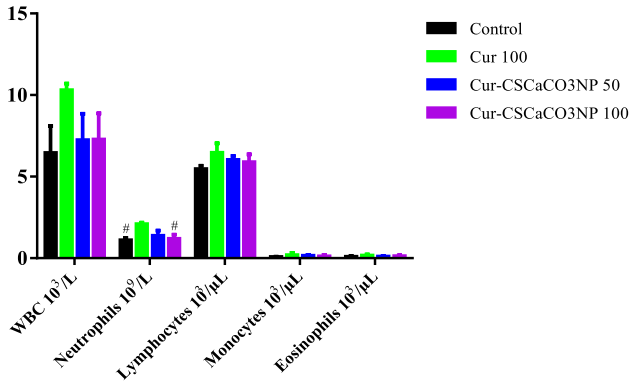

Fig. 6. Effect of Cur-CSCaCO$_3$NP and curcumin on leukogram in the blood of lead-administered rats. Values were presented as mean ± SEM, n = 5, # $P < 0.05$ vs Cur 100.

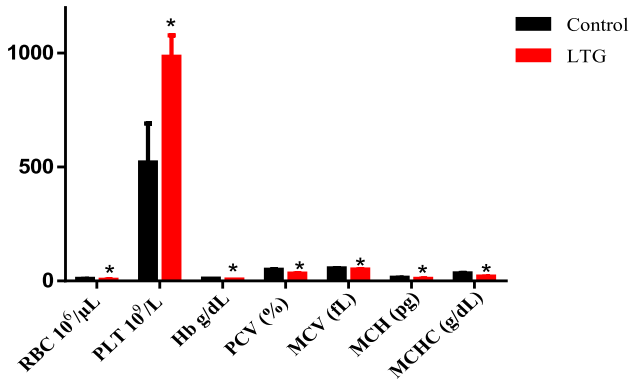

Fig. 7. Effects of lead on hematological values of rats after four weeks of induction. Values were presented as mean ± SEM, n = 5. *$P < 0.05$ vs control.

parameters in the rat's blood were analyzed using ANOVA [RBC: $F(3, 16) = 4.870$, $p = 0.0136$, Hb: $F(3, 16) = 4.659$, $p = 0.0159$] which showed statistically significant differences among the rat groups. Tukey's post hoc revealed statistically significant increase in the volume of rat's RBC in the control group (9.25 ± 0.23, $p = 0.0140$) and Cur-CSCaCO3NP 100 groups of rats (9.06 ± 0.15, $p = 0.0333$) when compared to the Cur 100 (7.78 ± 0.45) groups of rats. Further, a statistically significant increase was observed in the volume of Hb of the control group of rats (10.59 ± 0.13, $p = 0.0122$) when compared to the Cur 100 group of rats (8.678 ± 0.67). No statistically significant differences were observed in volumes of PLT, PCV, MCV, MCH and MCHC in all the treatment groups when compared to their control groups of rats (Fig. 8).

3.9. Effect of lead on SOD activities

The activity of SOD in the serum of the lead-administered rats revealed statistically significant differences as shown by the unpaired independent t-tests as follows; Serum [LTG (5.45 ± 1.14)] and the control group of rats (18.62 ± 0.16), $p = 0.0003$. These results showed that lead significantly decreased the SOD activity in the serum of the rats when compared to the control (Fig. 9).

3.10. Effect of Cur-CSCaCO$_3$NP on SOD activities

As shown in Fig. 10, the effect of Cur-CSCaCO$_3$NP and free curcumin on the SOD activities in the serum of lead-administered rats revealed statistically significant differences among the rat groups as shown by the one-way ANOVA [$F(3, 8) = 6.395$, $p = 0.0161$].

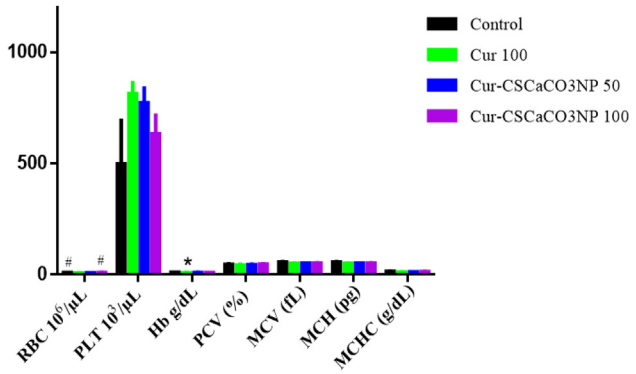

Fig. 8. Effects of Cur-CSCaCO$_3$NP and curcumin on hematological values of rats after 4 weeks of treatments. Values were presented as mean ± SEM, n = 5, *$p < 0.05$ vs control, # $P < 0.05$ vs Cur 100.

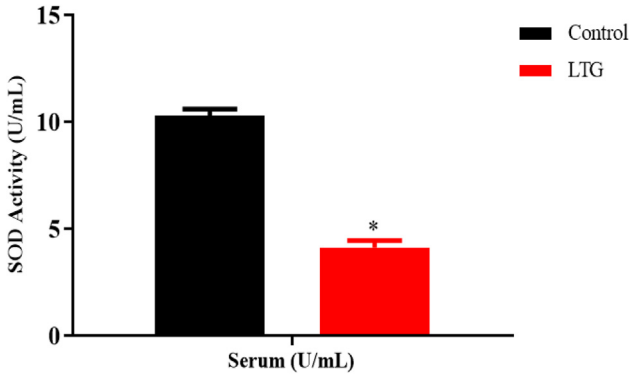

Fig. 9. Effect of lead on superoxide dismutase (SOD) activities in the serum of rats after 4 weeks of induction. Values were presented as mean ± SEM, n = 3. *$p < 0.05$ vs control.

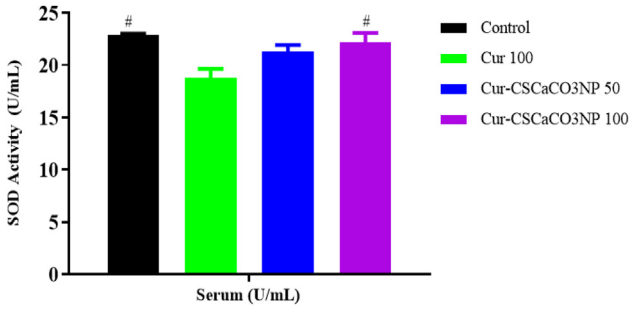

Fig. 10. Effect of Cur-CSCaCO$_3$NP and curcumin on superoxide dismutase (SOD) activities in the serum of lead-administered rats after 4 weeks of treatment. Values were presented as mean ± SEM, n = 3. # $p < 0.05$ vs Cur 100.

The Tukey's post hoc showed statistically significant increase of SOD activities in the serum of the control group (22.86 ± 0.16, $p = 0.0147$) and the serum of Cur-CSCaCO$_3$NP 100 groups of rats (22.17 ± 0.93, $p = 0.0381$) when compared to Cur 100 (18.79 ± 0.87).

3.11. Effect of lead on MDA level

The ELISA results for MDA level in the serum of the lead-administered rats revealed statistically significant differences among the means of various rat groups as shown by the unpaired independent t-tests as follows; Serum [LTG (25.53 ± 0.73)] and the control groups of rats (14.06 ± 1.83), $p = 0.0043$. These results

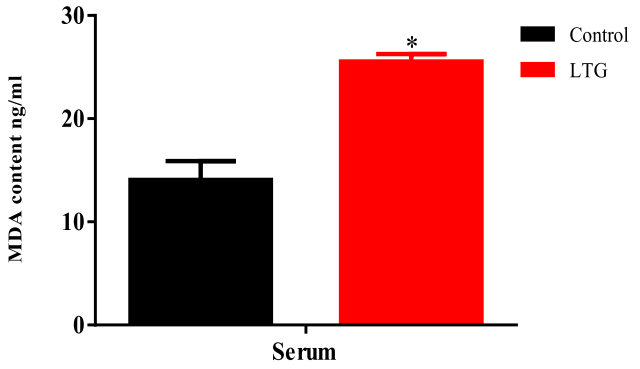

Fig. 11. Effect of lead on malondialdehyde (MDA) levels in the serum of rats after 4 weeks of induction. Values were presented as mean ± SEM, n = 3. *P < 0.05 vs control.

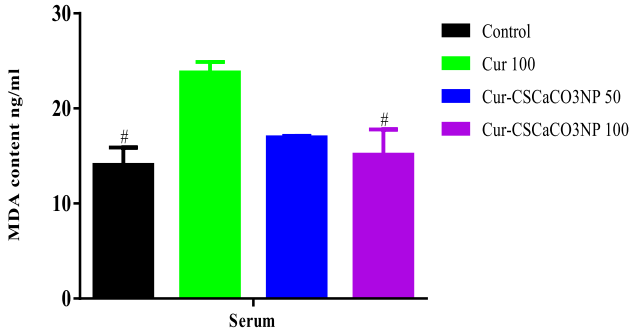

Fig. 12. Effect of Cur-CSCaCO$_3$NP and curcumin on malondialdehyde (MDA) levels in the serum of lead-administered rats after 4 weeks of treatment. Values were presented as mean ± SEM, n = 3, # P < 0.05 vs Cur 100.

showed that lead significantly increased the MDA levels in the serum of the lead-induced rats when compared to their control counterparts (Fig. 11).

3.12. Effect of Cur-CSCaCO$_3$NP on MDA level

As shown in Fig. 12, based on the ELISA results, one-way ANOVA revealed statistically significant differences of MDA levels in the serum among all the groups of rats [F (3, 8) = 6.605, p = 0.0148]. The Tukey's post hoc showed statistically significant decrease in MDA levels of the serum of control (14.06 ± 1.82, P = 0.0156) and the serum Cur-CSCaCO$_3$NP 100 groups of rats (15.14 ± 2.64, p = 0.0288), when compared to Cur 100 (23.79 ± 1.103).

3.13. Histopathology

3.13.1. Histological examination of the liver using H and E stain after lead-induction

Histopathological examination of the liver section from control rats revealed a normal hepatic architecture with well-defined central vein and hepatocytes with clear cytoplasm and prominent nucleus (Fig. 13A). However, liver sections from the LTG group of rats revealed some abnormalities as shown in Table 3 and Fig. 13B. Mann-Whitney U test showed significant differences (p < 0.05) of lesions observed for activated kupffer cells, sign of necrosis, fatty changes, karyolysis, pyknosis, karyorrhexis and inflammation in LTG group when compared to the control group.

3.13.2. Histological examination of the liver using H and E stain after treatment with Cur-CSCaCO$_3$NP

Histopathological examination of the liver section from control rats revealed a normal hepatic architecture (Fig. 14A). Although, the liver section from the Cur 100 group of rats revealed significant moderate changes in liver architecture and inflammations when compared to the control (Fig. 14B), restored liver architecture with no significant mild changes were observed in Cur-CSCaCO$_3$NP 50 and Cur-CSCaCO$_3$NP 100 groups of rats (Fig. 14C and 14D), when compared to the control group. Kruskal-Wallis, test for the global comparison between organ toxicity among groups was used. The result showed statistically significant differences (p < 0.05) of lesions observed for activated kupffer cells, sign of necrosis, fatty changes and karyolysis in Cur 100 group when compared to the control group. There was no statistically significant difference observed in Cur-CSCaCO$_3$NP 50 and Cur-CSCaCO$_3$NP 100 groups of rats when compared to the control (Table 4).

3.13.3. Histological examination of the kidney using H and E stain after lead-induction

Kidney section from the control group revealed a normal renal morphology consisting of a glomerulus and well-defined Bowman's capsule with adjacent proximal and distal convoluted

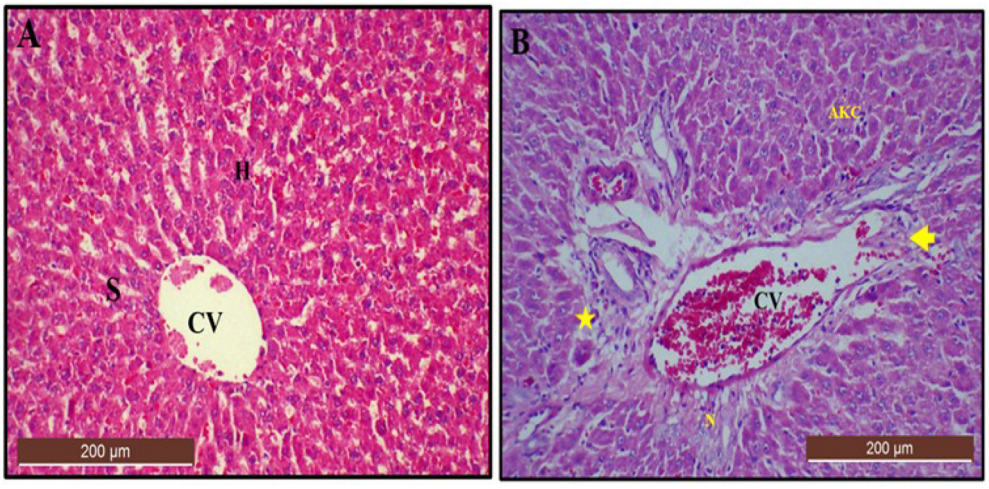

Fig. 13. Photomicrographs of liver section from rats treated with (A) Normal saline (control) showing normal hepatic architecture with central vain (CV), surrounding hepatocytes (H) and array of radiating sinusoids (S) (scored as 0). (B) 50 mg/kg of lead (LTG) showing congestion of central vain (*arrow*), fatty changes, foci of hepatic necrosis (N), pyknotic nuclei, infiltration of inflammatory cells (*star*) and numerous activated kupffer cells (AKC) (scored as 3). (H and E, X 10, scale bar = 200 µm).

Table 3
Scoring results of lesion in the liver of control and lead-administered rats after 4 weeks of lead-induction.

Pathological parameters	Control	LTG	Mann Whitney *U* test (p < value)
Activated Kupffer cells	0.4 ± 0.24	2.3 ± 0.2*	0.0079
Sign of necrosis	0.2 ± 0.2	2.5 ± 0.16*	0.0079
Vacuolation (fatty changes)	0.2 ± 0.2	2.6 ± 0.19*	0.0079
Inflammatory cell infiltration	0.2 ± 0.2	2.3 ± 0.26*	0.0079
Karyolysis	0.2 ± 0.2	2.3 ± 0.13*	0.0079
Pyknosis	0.2 ± 0.2	2.5 ± 0.16*	0.0079
Karyorrhexis	0.0	0.6 ± 0.24*	0.1667

The symbol * denotes the values were significantly different (p < 0.05) between lead-administered and the control groups of rats. Values were presented as mean ± SEM, n = 5.

tubules (Fig. 15A). The kidney section from the LTG group of rats showed some marked abnormalities as shown in Fig. 15B. Mann-Whitney *U* test showed significant differences (p < 0.05) of lesions observed for sign of necrosis, tubular dilatation, inflammatory cell, eosinophilic cytoplasm, atrophy of glomerulus and fatty degeneration in LTG group when compared to the control group (Table 5).

3.13.4. Histological examination of the kidney using H and e stain after treatment with Cur-CSCaCO$_3$NP

The light microscopy examination of the kidney section from control rats revealed a normal renal morphology (Fig. 16A). Although, the kidney section from the Cur 100 group of rats showed moderate congested hypercellular when compared to the control (Fig. 16B). Restored renal morphology with very mild changes were observed in Cur-CSCaCO$_3$NP 50 and Cur-CSCaCO$_3$NP 100 groups of rats (Fig. 16C and 16D), when compared to the control group. Kruskal-Wallis, test for the global comparison between organ toxicity among rats' groups was used. The result showed significant differences (p < 0.05) in lesions observed for sign of necrosis and fatty degeneration in Cur 100 group when compared to the control group. There was no statistically significant difference observed in Cur-CSCaCO$_3$NP 50 and Cur-CSCaCO$_3$NP 100 groups of rats when compared to the control (Table 6).

4. Discussion

The present study showed that lead induction in rats for four weeks revealed marked increased in the weight of the liver and kidney. Consequently, alterations of hematological parameters, oxidative stress and marked histopathological tissue abnormalities were observed in the rats' liver and kidneys. Similarly, lead induced pathological conditions related to redox homeostasis imbalance (Seddik et al., 2010), hematological alterations (Yu et al., 2004; Alwaleedi, 2016; Rehman et al., 2018), hepatic and renal dysfunctions (Amjad et al., 2013; Andjelkovic et al., 2019) were previously reported. However, in this study treatment with free curcumin to some extent reversed the aforementioned toxic insults induced by lead in the rats although, better ameliorative effects were observed with Cur-CSCaCO$_3$NP (50 mg/kg and 100 mg/kg). Further, significant ameliorations were best observed at higher dose of 100 mg/kg (Cur-CSCaCO$_3$NP 100) treatment than free curcumin against lead induced hepato-renal toxicity. This might be related to Cur-CSCaCO$_3$NP enhanced therapeutic efficacy than free curcumin which could be attributed to the nanoparticle's

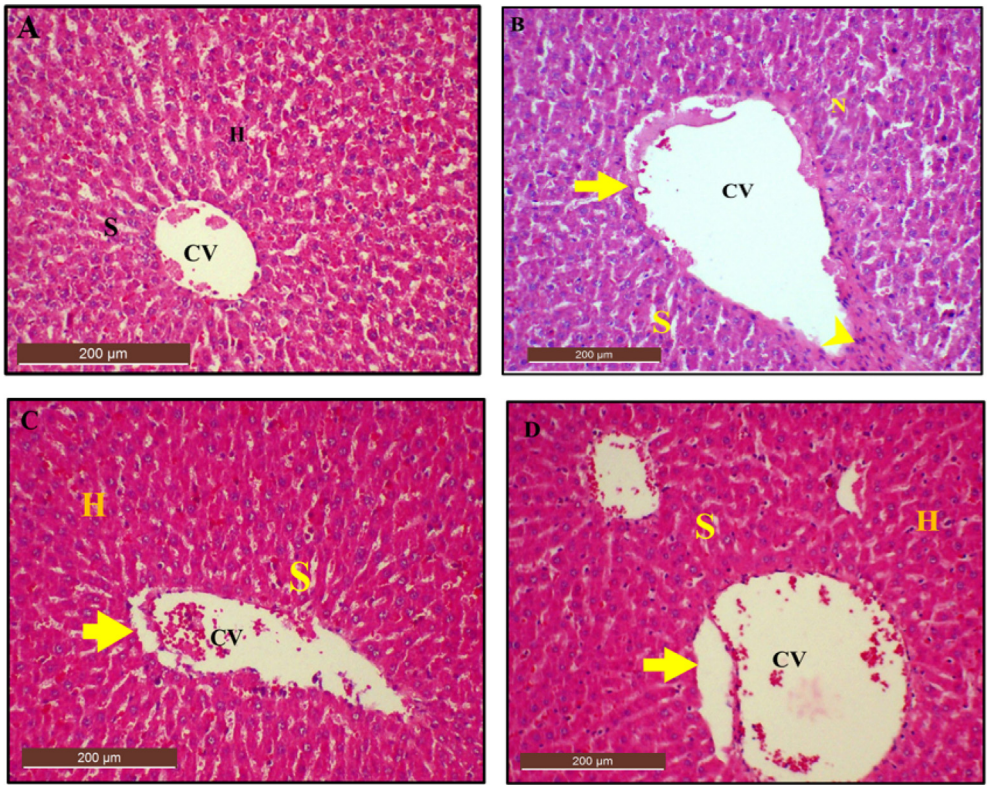

Fig. 14. Photomicrographs of liver section from rats treated with (A) Normal saline (control) showing normal liver architecture (scored as 0). (B) 100 mg/kg of curcumin (Cur 100) showing foci of hepatic necrosis (N) and infiltration of inflammatory cells (*yellow arrowhead*). (C) 50 mg/kg of Cur-CSCaCO$_3$NP (Cur-CSCaCO$_3$NP 50) and (D) 100 mg/kg of Cur-CSCaCO$_3$NP (Cur-CSCaCO$_3$NP 100) showing marked improved liver architecture and restoration of normal hepatocytes morphology and central vain (*green arrow*). (H and E, X10, scale bar = 200 µm).

Table 4
Scoring results of lesion in the liver of control and all the treated groups of rats after 4 weeks of treatment with curcumin and Cur-CSCaCO$_3$NP using Kruskal Wallis test for global comparison of organ lesions among all groups.

Pathological parameters	Control	Cur 100	Cur-CSCaCO$_3$NP 50	Cur-CSCaCO$_3$NP 100	Asymptomatic significant (p < value)
Activated Kupffer cells	0.4 ± 0.24	1.3 ± 0.12*	1.2 ± 0.12	1.1 + 0.1	0.0334
Necrosis	0.2 ± 0.2	1.4 ± 0.19*	1.2 ± 0.12	1.1 ± 0.1	0.0128
Vaculation (fatty changes)	0.4 ± 0.24	1.6 ± 0.19*	1.3 ± 0.2	1.1 ± 0.1	0.0159
Inflammatory cell infiltration	0.0	0.9 ± 0.24	0.8 ± 0.2	0.5 ± 0.32	0.0694
Karyolysis	0.2 ± 0.2	1.2 ± 0.2*	0.9 ± 0.1	0.6 ± 0.24	0.0303
Pyknosis	0.2 ± 0.2	1.1 ± 0.1	0.7 ± 0.3	0.6 ± 0.24	0.0965
Karyorrhexis	0.0	0.4 ± 0.24	0.3 ± 0.3	0.2 ± 0.2	0.5401

The symbol * denotes the values were significantly different (p < 0.05) between all the treated groups and the control group. Values were presented as mean ± SEM, n = 5.

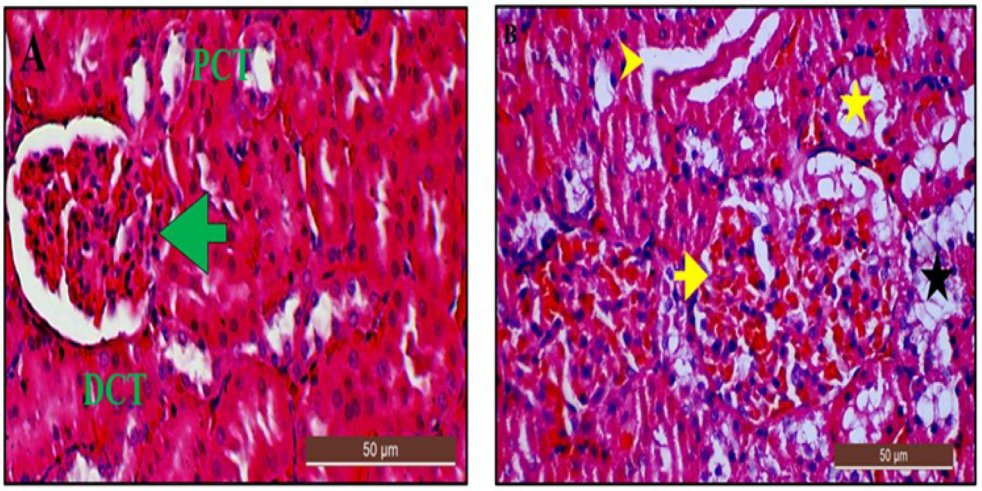

Fig. 15. Photomicrographs of kidney sections from rats treated with (A) Normal saline (control) showing normal histo-architecture with glomerulus (green arrow), proximal convoluted tubules (PCT) and distal convoluted tubules (DCT) (scored as 0). (B) 50 mg/kg of lead (LTG) showing congested hypercellular glomerulus (*yellow arrow*), prominent cytoplasmic vacuolation (fatty degeneration), cellular necrosis (*black star*) and glomerular atrophy, tubular dilatation (yellow arrowhead) and collapsed tubular tuft (*yellow star*) (scored as 3). (H and E, X40, scale bar = 50 µm).

Table 5
Scoring results of lesion in the kidney of control and lead-administered rats after 4 weeks of lead-induction.

Pathological parameters	Control	LTG	Mann Whitney *U* test (p < value)
Sign of Necrosis	0.1 ± 0.1	2.2 ± 0.12*	0.0079
Tubular dilatation	0.1 ± 0.1	1.9 ± 0.1*	0.0079
Inflammatory cell	0.1 ± 0.1	2.1 ± 0.33*	0.0079
Eosinophilic cytoplasm	0.3 ± 0.2	1.8 ± 0.37*	0.0238
Atrophy of glomerulus	0.2 ± 0.2	1.8 ± 0.26*	0.0159
Fatty degeneration	0.1 ± 0.1	2.8 ± 0.12*	0.0079

The symbol *denotes the values were significantly different (p < 0.05) between lead-administered group and the control group. Values were presented as mean ± SEM, n = 5.

ability to promote sustained and controlled drug release, enhanced cellular uptake and increased (5–9 fold) oral bioavailability in the body as stated by previous studies (Shaikh et al., 2009; Wang et al., 2012; Sankar et al., 2013).

In the current study, significant increase in the weights of lead administered rats' liver and kidneys were as a result of the tissue necrosis accompanied by fat depositions on the liver and kidney tissues causing an abnormal organ enlargement as further supported by this study's histopathology results. Fatty accumulations, kidney and liver enlargement in lead-induced toxicity were reported in previous literatures (Khan et al., 2008; Abdel Moneim et al., 2011; Yuan et al., 2014; Sun et al., 2017). However, treatment with free curcumin and Cur-CSCaCO$_3$NP showed restoration of normal organ weights due to the healing effect. Further, better healing effects were observed in the liver and kidneys of rats treated with high dose of Cur-CSCaCO$_3$NP. Similar results were also reported in the previous studies (El-Demerdash et al., 2009; Sankar et al., 2013; Salama et al., 2013; Soliman et al., 2015; Salahshoor et al., 2016; Marslin et al., 2018).

It is worthy to note that AST and ALT are key enzymes for several metabolic pathways present in the hepatic cells, which are widely used in the assessment of liver function. AST can be detected both in mitochondria and cytoplasm of cell while ALT is found only in the cytoplasm (Alwaleedi, 2015). This study indicated that lead-induced rats showed significant increase in the activities of ALP, AST, GGT, ALP and LDH, which are all signs of hepatic dysfunction and oxidative damage in the liver. This elevation observed in the enzymes activities is possibly due to cell fluidity and content leakage as a result of high metabolic rate and destructive alterations such as oxidative damage of hepatocytes as described by Omotoso et al. (2015) and Offor et al. (2017). The findings also concurred with the works of Ibrahim et al. (2012) and Offor et al. (2017) who reported the hepatotoxic effect of lead on liver hepatocytes resulting to an increase in the activities of AST and ALT disruption. In addition, Shalan et al. (2005), Salahshoor et al. (2016) and Alwaleedi, (2016) observed an increase in the serum level of GGT, ALP and LDH in lead intoxicated rats. The resultant decrease in albumin, globulin and TP observed in the current work, were in accordance with work of Lakshmi et al. (2013) and Saeed et al. (2017), who reported a significant reduction in the total protein, globulin and albumin in occupational lead exposed

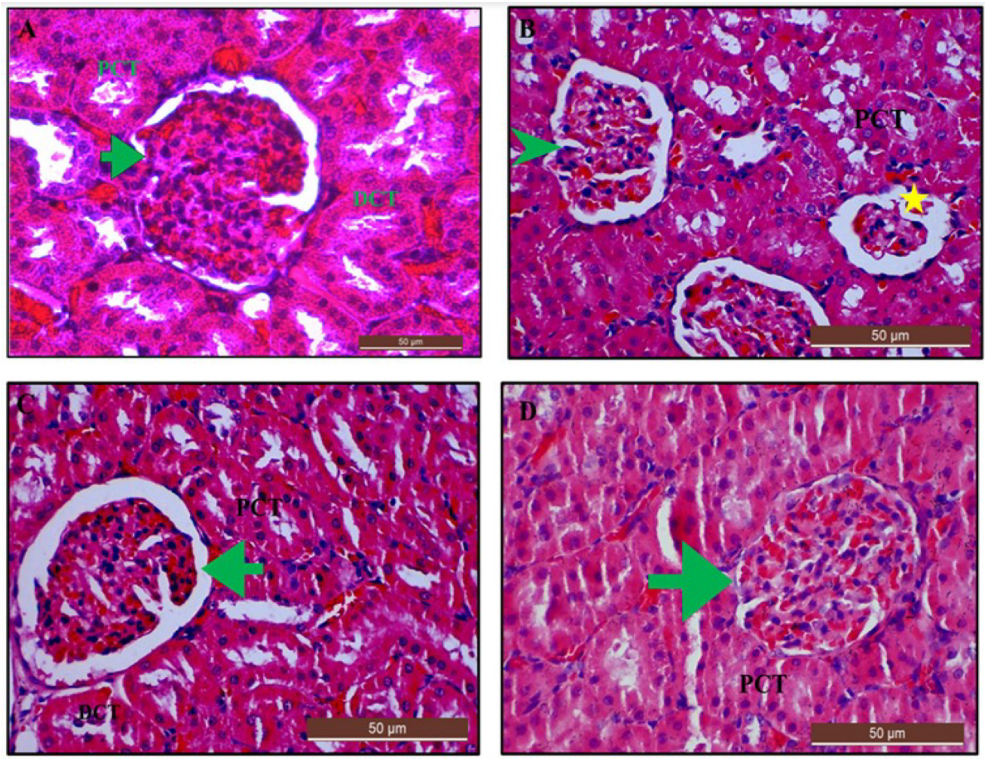

Fig. 16. Photomicrographs of kidney section from rats treated with (A) Normal saline (control) showing normal kidney architecture (scored as 0). (B) 100 mg/kg of curcumin (Cur 100) showing moderate congestion of glomerulus with inflammatory cells (green arrowhead) and glomerular atrophy (*yellow star*). (C) 50 mg/kg of Cur-CSCaCO$_3$NP (Cur-CSCaCO$_3$NP 50) and (D) 100 mg/kg of Cur-CSCaCO$_3$NP (Cur-CSCaCO$_3$NP 100) showing marked improved glomerular morphology and restoration of normal proximal and distal tubular architecture. (*green arrow*). (H and E, X40, scale bar = 50 µm).

Table 6
Scoring results of lesion in the kidney of control and all the treated groups of rats after 4 weeks of treatment with curcumin and Cur-CSCaCO$_3$NP using Kruskal Wallis test for global comparison of organ lesions.

Pathological parameters	Control	Cur 100	Cur-CSCaCO$_3$NP 50	Cur-CSCaCO$_3$NP 100	Asymptomatic significant ($p < 0.05$)
Necrosis	0.1 ± 0.1	1.1 ± 0.1*	1.8 ± 0.12	0.7 ± 0.2	0.0077
Tubular dilatation	1 ± 0.31	1.6 ± 0.1	1.2 ± 0.12	1.1 ± 0.1	0.7071
Inflammatory cell	0.1 ± 0.1	0.8 ± 0.26	0.4 ± 0.19	0.2 ± 0.12	0.1118
Eosinophilic cytoplasm	0.3 ± 0.2	1 ± 0.16	0.8 ± 0.12	0.6 ± 0.1	0.0573
Atrophy of glomerulus	0.2 ± 0.1	1.1 ± 0.29	0.8 ± 0.26	0.5 ± 0.16	0.0677
Fatty degeneration	0.1 ± 0.1	1 ± 0.16*	0.8 ± 0.16	0.5 ± 0.6	0.0126

The symbol * denotes the values were significantly different ($p < 0.05$) among all the treated groups and the control group. Values were presented as mean ± SEM, n = 5.

workers. Shalan et al. (2005) attributed these reductions to hepatic cell destruction due to lead intoxication. In the case of kidney function, the increase in the serum levels of blood creatinine and urea were also observed in this study, indicating a functional evidence of lead induced renal dysfunction. This is in accordance with previous literatures that reported increased levels of creatinine and urea, which are functional evidence of lead-induced nephrotoxicity (Missoun et al., 2010; Offor et al., 2017). However, administration of curcumin and Cur-CSCaCO$_3$NP in this study reversed the aforementioned alterations. These findings are in accordance with the previous literatures (Pari and Amali, 2005; Yousef et al., 2008; Al Kahtani et al., 2014; Abdel-Moneim et al., 2015; Abdel-Wahhab et al., 2016; Kushwaha et al., 2018).

This study revealed a significant decrease in RBC and hemoglobin in the blood of lead induced-rats which could be attributed to the lead toxic insults. Further, it might be due to the ability of lead to alter the cell metabolic activities, thereby destructing the calcium influx and causing possible inhibition of some enzymatic activities, which are useful in heme biosynthesis as reported by Alwaleedi, (2015) and Andjelkovic et al. (2019). Thus, lead could possibly bind to RBCs to irritate the cell membrane resulting to RBCs destruction (Varnai et al., 2004; Alwaleedi, 2016; Gani et al., 2017). In addition, the current study showed an increased level of total bilirubin. This could be due to lead-induced heme catabolism thus, possibly enhanced the activity of heme oxygenase in conversion of heme to bilirubin as reported by Offor et al. (2017). In addition, these findings are in agreement with the work of Suradkar et al. (2009), who reported acute disruption in the biosynthesis of heme due to the ability of lead to obstruct the activities of cytoplasmic and mitochondrial enzymes. Lead was reported to counteract the effect of some enzymes responsible for the production of Hb thereby decreasing erythrocytes life span (Ibrahim et al., 2012; Velaga et al., 2014). In this study, an increased number of RBC and hemoglobin with a resultant decreased level of total bilirubin was observed in rats administered with curcumin and Cur-CSCaCO$_3$NP, although, a better therapeutic effect was observed with Cur-CSCaCO$_3$NP treatment. Previous studies have reported similar findings and attributed it to anti-inflammatory and therapeutic properties of curcumin on hematological parameters (Motterlini et al., 2000; Yousef et al., 2008;

Abdel-Moneim et al., 2015; Hossen et al., 2017; Hussain et al., 2017).

The current study revealed significant decrease in PCV, MCV, MCH and MCHC in lead administered rats. These alterations could be due to the cellular disruption caused by the toxic effect of lead. Similar findings were seen in the work of Andjelkovic et al. (2019) who reported the concordant hematological alterations resulting to acute normocytic normochromic anemia attributed to lead-induced oxidative stress. The resultant increase in WBC, platelets, neutrophils, lymphocytes and eosinophils observed in this study, could be as a result of the lead-induced inflammations, which is in line with the work of other authors (Ibrahim et al., 2012; Fosu-Mensah et al., 2017; Andjelkovic et al., 2019). However, a decrease in PCV, MCV, MCH and MCHC with a resultant increase in the WBC, platelets, neutrophils, lymphocytes and eosinophils were observed in rats administered with curcumin and Cur-CSCaCO$_3$NP. Further, Cur-CSCaCO$_3$NP demonstrated a better therapeutic effect compared to free curcumin. This reversal could be attributed to anti-inflammatory and immune-modulatory properties of curcumin as documented in previous literatures (Soliman et al., 2015; Hossen et al., 2017; Hussain et al., 2017; Saeed et al., 2017).

Oxidative stress occurs when there is an imbalance homeostasis between free radicals and the ability of the biological system to readily detoxify the highly generated intermediate reactive species which could lead to general tissue damage (Patra et al., 2011). Lead causes oxidative stress via two different pathways operative simultaneously; Initial generation of ROS then the depletion of the system's antioxidant reserves (Patrick, 2006). These generated ROS causes series of cell damages via different mechanisms due to the resulted redox imbalance which in turn produces series of harmful effects to functional organs such as liver and kidneys (Soliman et al., 2015). In the present study, significant decrease in the SOD activities and increase in the MDA levels in the lead-induced rats' serum were observed. These findings suggested that toxic effect of lead resulted to oxidative stress which concurs with previous literatures (Farooq et al., 2013; Lakshmi et al., 2013; Nadia, 2013; Andjelkovic et al., 2019). It is worthy to note that active body antioxidants such as SOD plays an important role in nullifying the generated ROS (Flora et al., 2012). Curcumin operates primarily via antioxidant mechanism to alleviate oxidative stress biomarkers by enhancing the activities of antioxidant enzymes such as SOD, GSH and CAT (Sahebkar et al., 2015; Liu et al., 2016). In this study, treatment with Cur-CSCaCO$_3$NP significantly increased the activities of SOD and conversely decreased the MDA levels when compared to free curcumin treatment. Although, antioxidant effect that resulted to these reversals was better observed in high dose of Cur-CSCaCO$_3$NP treatment. These findings are in accordance with the work the previous works on both antioxidant effect of free curcumin and nanoconjugated curcumin (Yadav et al., 2012; Flora et al., 2013; Sankar et al., 2013; Ansar et al., 2019).

In the present study, the light microscopic analysis of the liver revealed histological alterations characterized by congested central vein with cellular infiltrations, fatty changes and necrotic hepatocytes. The lesion scoring revealed significant increase in multiple pathological parameters observed when compared to the control. These histopathological changes could be attributed to the ability of lead to induce oxidative stress as observed in the

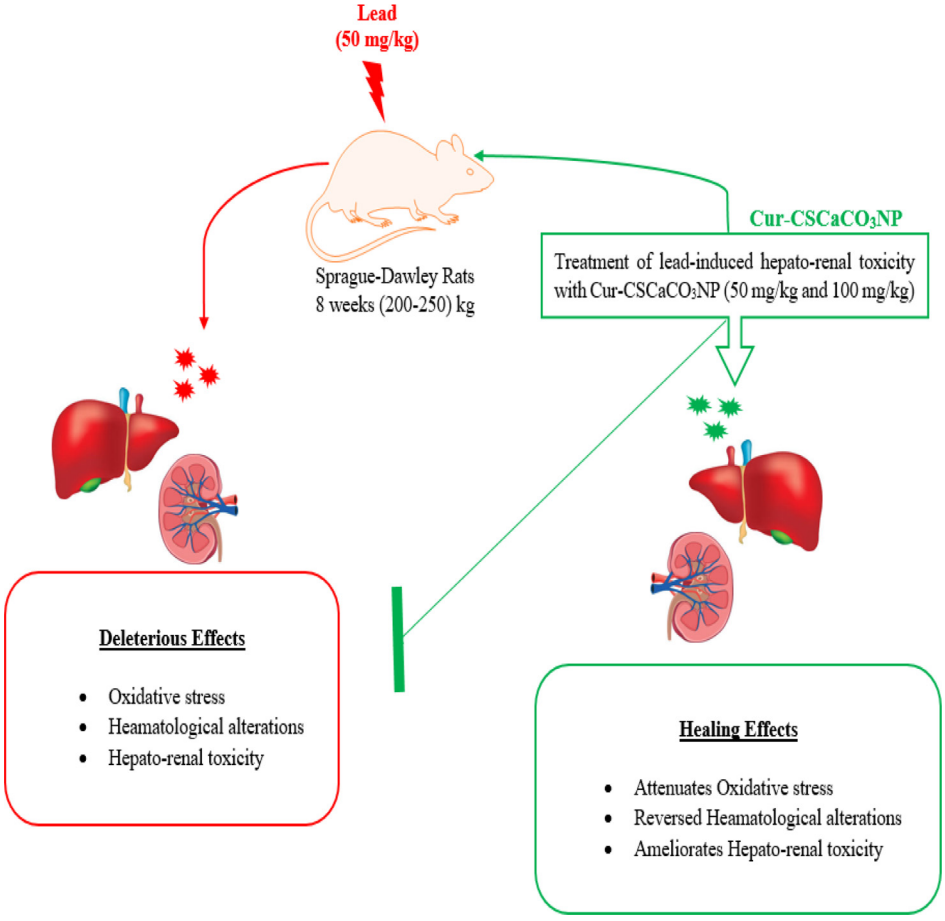

Fig. 17. Proposed mechanism of lead-induced hepato-renal toxicity and the ameliorative effects of Cur-CSCaCO$_3$NP. Note: curcumin-loaded cockle shell derived calcium carbonate nanoparticles (Cur-CSCaCO$_3$NP).

current study and inflammations, lipid peroxidation and oxidative stress as reported in previous literatures (Sharma et al., 2009; Omotoso et al., 2015). In addition, the renal microscopic examination in the current study showed glomerular atrophy, collapsed tubular tuft and fatty degenerations. The lesion scoring method revealed significant increase in multiple pathological parameters observed when compared to the control. This renal histopathological alterations observed are similar with the findings of previous studies (Massanyi et al., 2007; Nisar et al., 2011; Yuan et al., 2014). Consequently, these morphological alterations observed in both liver and kidney in this study could be due to the toxic insults of lead resulting to hepato-renal damages. In this study, liver and kidney sections of rats that were administered free curcumin showed a mild change in liver and kidney architecture compared to LTG groups of rats. In addition, it is worthy to know that there were no obvious changes observed in the liver and kidney sections of rats treated with Cur-CSCaCO$_3$NP irrespective of the dose given when compared to their respective control groups. This indicates a better efficacy of Cur-CSCaCO$_3$NP as compared to free curcumin. Findings from this study are in accordance with previous studies that reported the beneficial effect of free curcumin with enhanced therapeutic effect of different nanoconjugated curcumin in hepato-renal injury (Ghoniem et al., 2012; Gao et al., 2013; Abdel-Wahhab et al., 2016; Maithilikarpagaselvi et al., 2016; Marslin et al., 2018; Ansar et al., 2019; Li et al., 2019).

5. Conclusion

This study has proven that the administration of lead in rats for four weeks can induce oxidative stress, hematological alterations, histopathological aberrations as well as failure in the liver and kidney functions (Fig. 17). However, treatment with free curcumin and Cur-CSCaCO$_3$NP demonstrated some therapeutic effects by reversing the aforementioned conditions as demonstrated in Fig. 17. Although the rats treated with free curcumin showed some ameliorative effects, Cur-CSCaCO$_3$NP treatment demonstrated enhanced/better ameliorative effects through significant improvements on the histopathological aberrations, hematological parameters, increased SOD activities and decreased MDA levels, when compared to free curcumin treatment. Interestingly, Cur-CSCaCO$_3$NP at high dose displayed a greater efficacy for the treatment of lead-induced hepato-renal toxicity when compared to its equivalent free curcumin dose. Noteworthy, to some extent this study also revealed a better therapeutic efficacy of Cur-CSCaCO$_3$NP at a lower dose when compared to high dose of free curcumin. Thus, it can be concluded that CSCaCO$_3$NP can be applicable for targeted delivery of curcumin (antioxidant) for the oral treatment of lead-induced hepato-renal toxicity. In addition, the idea on the use of cockle shells as a source of calcium carbonate nanoparticle may help in a significant reduction of abundant waste materials generated thereby improving and promoting environmental waste recycling. Although, this study investigated SOD activities and MDA levels on lead-induced hepato-renal toxicity in rats to assess the antioxidant effects of Cur-CSCaCO$_3$NP, further studies should be carried out to decipher the antioxidant effects of Cur-CSCaCO$_3$NP on other oxidative stress biomarkers such as GSH, glutathione reductase, glutathione peroxidase and catalase. This might provide additional clue on the mechanism behind the antioxidant effect of Cur-CSCaCO$_3$NP.

Declaration of Competing Interest

The authors declare that they have no known competing financial interests or personal relationships that could have appeared to influence the work reported in this paper.

Acknowledgement

The authors will like to acknowledge Ministry of Higher Education and Universiti Putra Malaysia for funding this research (KPT FRGS and GP-IPS 9663600).

References

Abdel-Moneim, A.M., El-Toweissy, M.Y., Ali, A.M., Awad Allah, A.A.M., Darwish, H.S., Sadek, I.A., 2015. Curcumin ameliorates Lead (Pb2+)-induced hemato-biochemical alterations and renal oxidative damage in a rat model. Biol. Trace Elem. Res. 168, 206–220. https://doi.org/10.1007/s12011-015-0360-1.

Abdel-Wahhab, M.A., Salman, A.S., Ibrahim, M.I.M., El-Kady, A.A., Abdel-Aziem, S.H., Hassan, N.S., Waly, A.I., 2016. Curcumin nanoparticles loaded hydrogels protects against aflatoxin B1-induced genotoxicity in rat liver. Food Chem. Toxicol. 94, 159–171. https://doi.org/10.1016/j.fct.2016.06.005.

Abdel Moneim, A.E., Dkhil, M.A., Al-Quraishy, S., 2011. The protective effect of flaxseed oil on lead acetate-induced renal toxicity in rats. J. Hazard. Mater. 194, 250–255. https://doi.org/10.1016/j.jhazmat.2011.07.097.

Abu-taweel, G.M., 2018. Curcumin attenuates lead (Pb)–induced neurobehaviorl and neurobiochemical dysfunction: a review. Int. J. Pharm. Pharm. Sci. 10, 23. https://doi.org/10.22159/ijpps.2018v10i8.27191.

Agarwal, R., Goel, S.K., Behari, J.R., 2010. Detoxification and antioxidant effects of curcumin in rats experimentally exposed to mercury. J. Appl. Toxicol. 30, 457–468. https://doi.org/10.1002/jat.1517.

Al Kahtani, M.A., Abdel-Moneim, A.M., El-Sayed, W.M., 2014. The influence of taurine pretreatment on aluminum chloride induced nephrotoxicity in Swiss albino mice. Histol. Histopathol. 29, 45–55.

Alwaleedi, S.A., 2016. Hematobiochemical changes induced by lead intoxication in male and female albinomice. Natl. J. Physiol. Pharm. Pharmacol. 6, 46–51. https://doi.org/10.5455/njppp.2015.5.0910201578.

Alwaleedi, S.A., 2015. Haemato-biochemical changes induced by lead intoxication in male and female albino mice. Int. J. Recent Sci. Res. 6, 3999–4004.

Amjad, Z., Iqbal, M.Z., Shoro, A.A., 2013. Biochemistry & physiology : open access lead-induced reduction in body and kidney weight of wistar albino rats ameliorated by ginkgo biloba extract (EGb 761). Biochem. Physiol. 2, 2–5. https://doi.org/10.4172/2168-9652.1000113.

Andjelkovic, M., Djordjevic, A.B., Antonijevic, E., Spasojevic-kalimanovska, V., Jovanovic, M., Boricic, N., 2019. Toxic effect of acute cadmium and lead exposure in rat blood, liver, and kidney. Int. J. Environ. Res. Public Health 16, 274. https://doi.org/10.3390/ijerph16020274.

Ansar, S., Farhat, S., Abudawood, M., Hamed, S., 2019. Effect of curcumin and curcumin nanoparticles against lead induced. Biomed. Res. 30, 57–60.

Ayuba Y, Ekanem A. U, G.S.H., 2017. Effect of Oral Administration of Lead Acetate Exposure on the Histology of the Testis and Testicular Sperm Concentration in Wistar Albino Rats. Sch. J. Appl. Med. Sci. 1, 2337–2344. Doi: 10.21276/sjams

Bhattacharjee, A., Kulkarni, V.H., Habbu, P.V., Chakraborty, M., 2018. Detrimental effects of lead on human health and protective effect by natural polyphenols: a review. Int. Res. J. Pharm. 9, 4–13. https://doi.org/10.7897/2230-8407.09681.

Bose-O'Reilly, S., Yabe, J., Makumba, J., Schutzmeier, P., Ericson, B., Caravanos, J., 2017. Lead intoxicated children in Kabwe. Zambia. Environ. Res. 165, 420–424. https://doi.org/10.1016/j.envres.2017.10.024.

Chirio, D., Peira, E., Dianzani, C., Muntoni, E., Gigliotti, C., Ferrara, B., Sapino, S., Chindamo, G., Gallarate, M., 2019. Development of Solid Lipid Nanoparticles by Cold Dilution of Microemulsions: Curcumin Loading, Preliminary In Vitro Studies, and Biodistribution. Nanomaterials 9, 230. https://doi.org/10.3390/nano9020230.

Danmaigoro, A., Selvarajah, G.T., Mohd Noor, M.H., Mahmud, R., Abu Bakar, M.Z., 2018. Toxicity and safety evaluation of doxorubicin-loaded cockleshell-derived calcium carbonate nanoparticle in dogs. Adv. Pharmacol. Sci. 2018. https://doi.org/10.1155/2018/4848602.

Danmaigoro, A., Selvarajah, G.T., Noor, M.H.M., Mahmud, R., Zakaria, M.Z.A.B., 2017. Development of cockleshell (Anadara granosa) derived CaCO3nanoparticle for doxorubicin delivery. J. Comput. Theor. Nanosci. 14, 5074–5086. https://doi.org/10.1166/jctn.2017.6920.

El-Demerdash, F.M., Yousef, M.I., Radwan, F.M.E., 2009. Ameliorating effect of curcumin on sodium arsenite-induced oxidative damage and lipid peroxidation in different rat organs. Food Chem. Toxicol. 47, 249–254. https://doi.org/10.1016/j.fct.2008.11.013.

Farooq, Y., Mazhar Hussain, M., Bin Aleem, S., 2013. Evaluation of oxidative stress, liver functions and anemia in lead intoxicated Sprague Dawley rats. Rawal Med. J. 38, 181–183.

Flora, G., Gupta, D., Tiwari, A., 2013. Preventive efficacy of bulk and nanocurcumin against lead-induced oxidative stress in mice. Biol. Trace Elem. Res. 152, 31–40. https://doi.org/10.1007/s12011-012-9586-3.

Flora, G., Gupta, D., Tiwari, A., 2012. Toxicity of lead: A review with recent updates. Interdiscip. Toxicol. 5, 47–58. https://doi.org/10.2478/v10102-012-0009-2.

Fosu-Mensah, B.Y., Addae, E., Yirenya-Tawiah, D., Nyame, F., 2017. Heavy metals concentration and distribution in soils and vegetation at Korle Lagoon area in Accra. Ghana. Cogent Environ. Sci. 3, 1–14. https://doi.org/10.1080/23311843.2017.1405887.

Fu, W., Mohd Noor, M.H., Yusof, L.M., Ibrahim, T.A.T., Keong, Y.S., Jaji, A.Z., Zakaria, M.Z.A.B., 2017. In vitro evaluation of a novel pH sensitive drug delivery system

based cockle shell-derived aragonite nanoparticles against osteosarcoma. J. Exp. Nanosci. 1–22. https://doi.org/10.1080/17458080.2017.1287965.
Gani, M.U., Siddiqui, M.S.I., Islam, K., Ahmed, S., Mostofa, M., 2017. Study on Hematological Alter Ations in Experimental Lead Toxicosis in Long Evans. Malaysian J. vetrinary Res. 8, 11–18.
Gao, S., Duan, X., Wang, X., Dong, D., Liu, D., Li, X., Sun, G., Li, B., 2013. Curcumin attenuates arsenic-induced hepatic injuries and oxidative stress in experimental mice through activation of Nrf2 pathway, promotion of arsenic methylation and urinary excretion. Food Chem. Toxicol. 59, 739–747. https://doi.org/10.1016/j.fct.2013.07.032.
García-Niño, W.R., Pedraza-Chaverrí, J., 2014. Protective effect of curcumin against heavy metals-induced liver damage. Food Chem. Toxicol. 69, 182–201. https://doi.org/10.1016/j.fct.2014.04.016.
Ghoniem, M.H., El-sharkawy, N.I., Hussein, M.M.A., Moustafa, G.G., 2012. Efficacy of Curcumin on Lead Induced Nephrotoxicity in Female Albino Rats. J. Am. Sci., 8
Giner-Casares, J.J., Henriksen-Lacey, M., Coronado-Puchau, M., Liz-Marzán, L.M., 2016. Inorganic nanoparticles for biomedicine: where materials scientists meet medical research. Mater. Today 19, 19–28. https://doi.org/10.1016/j.mattod.2015.07.004.
Hae, S.L., Ki, K.J., Jae, Y.C., Man, H.R., Hong, S., Kwon, M., Seung, H.K., Seog, Y.K., 2007. Neuroprotective effect of curcumin is mainly mediated by blockade of microglial cell activation. Pharmazie 62, 937–942. https://doi.org/10.1691/ph.2007.12.7563.
Haleagrahara, N., Chakravarthi, S., Kulur, A.B., 2011. Effects of chronic lead acetate exposure on bone marrow lipid peroxidation and antioxidant enzyme activities in rats. African J. Pharm. Pharmacol. 5, 923–929. https://doi.org/10.5897/AJPP10.173.
Hamidu, A., Mokrish, A., Mansor, R., Shameha, I., Razak, A., Danmaigoro, A., Jaji, A.Z., Bakar, Z.A., 2019. Modi fi ed methods of nanoparticles synthesis in pH-sensitive nano-carriers production for doxorubicin delivery on MCF-7 breast cancer cell line. Int. J. Nanomedicine 14, 3615–3627.
Hammadi, N.I., Abba, Y., Hezmee, M.N.M., Razak, I.S.A., Jaji, A.Z., Isa, T., Mahmood, S. K., Zakaria, M.Z.A.B., 2017. Formulation of a sustained release docetaxel loaded cockle shell-derived calcium carbonate nanoparticles against breast cancer. Pharm. Res. 34, 1193–1203. https://doi.org/10.1007/s11095-017-2135-1.
Hossen, M.S., Tanvir, E.M., Prince, M.B., Paul, S., Saha, M., Ali, M.Y., Gan, S.H., Khalil, M.I., Karim, N., 2017. Protective mechanism of turmeric (Curcuma longa) on carbofuran-induced hematological and hepatic toxicities in a rat model. Pharm. Biol. 55, 1937–1945. https://doi.org/10.1080/13880209.2017.1345951.
Husain, S.M.D., 2015. NeurohistologicalEffects of Lead on Cerebellum of Adult Albimo Rat Dr S M Dawar Husain Medical Science. Int. J. Sci. Res. 4, 2277–8179.
Hussain, M.A., Hassan, B.B., Masoud, R.E., Al Tamany, D., 2017. Curcumin attenuates erythropoiesis in recombinant human erythropoietin-induced polycythemia in rats. Natl. J. Physiol. Pharm. Pharmacol. 7, 766–770. https://doi.org/10.5455/njppp.2017.7.0306214032017.
Ibrahim, N.M., Eweis, E.A., El-Beltagi, H.S., Abdel-Mobdy, Y.E., 2012. Effect of lead acetate toxicity on experimental male albino rat. Asian Pac. J. Trop. Biomed. 2, 41–46. https://doi.org/10.1016/S2221-1691(11)60187-1.
IHME, 2017. Institute for Health Metrics and Evaluation (IHME). University of Washington. GBD Comp. Seattle, WA IHME.
Isa, T., Zakaria, Z.A.B., Rukayadi, Y., Hezmee, M.N.M., Jaji, A.Z., Imam, M.U., Hammadi, N.I., Mahmood, S.K., 2016. Antibacterial activity of ciprofloxacin-encapsulated cockle shells calcium carbonate (Aragonite) nanoparticles and its biocompatability in macrophage J774A.1. Int. J. Mol. Sci. 17. https://doi.org/10.3390/ijms17050713.
Jacobs, D., Clickner, R., Zhou, J., Viet, S., Marker, D., Rogers, J., Zeldin, D., Broene, P., Friedman, W., 2002. The prevalence of lead-based paint hazards in U.S housing. (Children's Health Articles). Environ. Health Perspect. 110, A599.
Jaji, A.Z., Zakaria, Z.A.B., Mahmud, R., Loqman, M.Y., Hezmee, M.N.M., Abba, Y., Isa, T., Mahmood, S.K., 2017. Safety assessments of subcutaneous doses of aragonite calcium carbonate nanocrystals in rats. J. Nanoparticle Res. 19, 175. https://doi.org/10.1007/s11051-017-3849-z.
Jarvis, P., Quy, K., Macadam, J., Edwards, M., Smith, M., 2018. Intake of lead (Pb) from tap water of homes with leaded and low lead plumbing systems. Sci. Total Environ. 644, 1346–1356. https://doi.org/10.1016/j.scitotenv.2018.07.064.
Kabeer, A., Mailafiya, M.M., Danmaigoro, A., Rahim, E.A., Bakar, Z.A., 2019. Therapeutic potential of curcumin against lead-induced toxicity : A review. Biomed. Res. Ther. 6, 3053–3066.
Kamba, A.S., Ismail, M., Azmi Tengku Ibrahim, T., Zakaria, Z.A.B., 2014. Biocompatibility of bio based calcium carbonate nanocrystals aragonite polymorph on nih 3T3 fibroblast cell line. African J. Tradit. Complement. Altern. Med. 11, 31–38. Doi: 10.4314/ajtcam.v11i4.5
Khan, M.S.H., Mostofa, M., Jahan, M.S., Sayed, M.A., Hossain, M.A., 2008. Effect of garlic and vitamin B-complex in lead acetate induced toxicities in mice. Bangladesh J. Vet. Med. 6, 203–210.
Kim, J., Lee, Y., Yang, M., 2014. Environmental exposure to lead (Pb) and variations in its susceptibility. J. Environ. Sci. Heal. - Part C Environ. Carcinog. Ecotoxicol. Rev. 32, 159–185. https://doi.org/10.1080/10590501.2014.907461.
Kushwaha, P., Yadav, A., Samim, M., Flora, S.J.S., 2018. Combinatorial drug delivery strategy employing nano-curcumin and nano-MiADMSA for the treatment of arsenic intoxication in mouse. Chem. Biol. Interact. 286, 78–87. https://doi.org/10.1016/j.cbi.2018.03.006.
Lakshmi, B.V.S., Sudhakar, M., Aparna, M., 2013. Protective potential of Black grapes against lead induced oxidative stress in rats. Environ. Toxicol. Pharmacol. 35, 361–368. https://doi.org/10.1016/j.etap.2013.01.008.
Li, J., Niu, R., Dong, L., Gao, L., Zhang, J., Zheng, Y., Shi, M., Liu, Z., Li, K., 2019. Nanoencapsulation of Curcumin and Its Protective Effects against CCl 4 - Induced Hepatotoxicity in Mice 2019.
Liu, W., Zhai, Y., Heng, X., Che, F.Y., Chen, W., Sun, D., Zhai, G., 2016. Oral bioavailability of curcumin: problems and advancements. J. Drug Target. 24, 694–702. https://doi.org/10.3109/1061186X.2016.1157883.
Mailafiya, M.M., Abubakar, K., Danmaigoro, A., Chiroma, S.M., Bin, E., Rahim, A., Aris, M., Moklas, M., 2019a. Cockle shell-derived calcium carbonate (aragonite) nanoparticles : a dynamite to nanomedicine. Appl. Sci. 9, 2894.
Mailafiya, M.M., Abubakar, K., Danmaigoro, A., Chiroma, S.M., Bin, E., Rahim, A., Aris, M., Moklas, M., Abu, Z., Zakaria, B., 2019b. Evaluation of in vitro release kinetics and mechanisms of curcumin-loaded cockle shell-derived calcium carbonate nanoparticles. Biomed. Res. Ther. 6, 3518–3540.
Mailafiya, M.M., Aris, M., Moklas, M., Abubakar, K., Danmaigoro, A., Chiroma, S.M., Bin, E., Rahim, A., Abu, Z., Zakaria, B., 2019c. Cytotoxicity studies of curcumin loaded-cockle shell-derived calcium carbonate nanoparticles. Nanosci. Nanotechnology-Asia 9, 1–7. https://doi.org/10.2174/2210681209666191128155819.
Maithilikarpagaselvi, N., Sridhar, M.G., Swaminathan, R.P., Sripradha, R., Badhe, B., 2016. Curcumin inhibits hyperlipidemia and hepatic fat accumulation in high-fructose-fed male Wistar rats. Pharm. Biol. 54, 2857–2863. https://doi.org/10.1080/13880209.2016.1187179.
Marslin, G., Prakash, J., Qi, S., Franklin, G., 2018. Oral delivery of curcumin polymeric nanoparticles ameliorates CCl4-induced subacute hepatotoxicity in wistar rats. Polymers (Basel). 10, 541. https://doi.org/10.3390/polym10050541.
Mason, L.H., Harp, J.P., Han, D.Y., 2014. Pb neurotoxicity: neuropsychological effects of lead toxicity. Biomed Res. Int. 2014, 840547. https://doi.org/10.1155/2014/840547.
Massanyi, P., Lukac, N., Makarevich, A.V., Chrenek, P., Forgacs, Z., Zakrzewski, M., Stawarz, R., Toman, R., Lazor, P., Flesarova, S., 2007. Lead-induced alterations in rat kidneys and testes in vivo. J. Environ. Sci. Heal. - Part A Toxic/Hazardous Subst. Environ. Eng. 42, 671–676. https://doi.org/10.1080/10934520701244474.
Missoun, F., Slimani, M., Aoues, A., 2010. Toxic effect of lead on kidney function in rat Wistar. African J. Biochem. Res. 4, 21–27.
Motterlini, R., Foresti, R., Bassi, R., Green, C.J., 2000. Curcumin, an antioxidant and anti-inflammatory agent, induces heme oxygenase-1 and protects endothelial cells against oxidative stress. Free Radic. Biol. Med. 28, 1303–1312. https://doi.org/10.1016/S0891-5849(00)00294-X.
Nadia Asyura, S.N., Hamzah, H., Shaari, R.M., 2016. Blood profiles and histopathological changes of liver and kidney tissues from male sprague dawley rats treated with ethanol extracts of clinacanthus nutans leaf. J. Clin. Toxicol. 06. https://doi.org/10.4172/2161-0495.1000329.
Nadia, N.O., 2013. The role of antioxidant properties of Celery against lead acetate induced hepatotoxicity and oxidative stress in irradiated rats. Arab. J. Nucl. Sci. Appli 46, 339–346.
Nisar, M.F., Nasir, I., Shaheen, S., Khalid, A., Tazeen, N., 2011. Chronic lead acetate nephrotoxicity: a histological study on albino rats. Ann. King Edward Med. Univ. 17, 239.
Nurul, S.A.S., Hazilawati, H., Mohd, R.S., Mohd, F.H.R., Noordin, M.M., Norhaizan, M. E., 2018. Subacute oral toxicity assesment of ethanol extract of mariposa christia vespertilionis leaves in male sprague dawley rats. Toxicol. Res. 34, 85–95. https://doi.org/10.5487/TR.2018.34.2.085.
Offor, S.J., Mbagwu, H.O.C., Orisakwe, O.E., 2017. Lead induced hepato-renal damage in male albino rats and effects of activated charcoal. Front. Pharmacol. 8, 1–10. https://doi.org/10.3389/fphar.2017.00107.
Omotoso, B.R., Abiodun, A.A., Ijomone, O.M., Adewole, S.O., 2015. Lead-induced damage on hepatocytes and hepatic reticular fibres in rats; protective role of aqueous extract of moringa oleifera leaves (Lam). J. Biosci. Med. 03, 27–35. https://doi.org/10.4236/jbm.2015.35004.
Owolabi JO, O.E. and C.-M.E., 2012. Healing and Prophylactic Effects of Moringa oleifera Leaf Extract on Lead Induced Damage to Haematological and Bone Marrow Elements in Adult Wistar Rat Models. Open Access Sci. Reports 1, 386. Doi: 10.4172/scientificreports.
Sankar, Palanisamy, Telang, Avinash Gopal, Kalaivanan, Ramya, Karunakaran, Vijayakaran, Kesavan Manikam, S.N.S., 2013. Effects of nanoparticle-encapsulated curcumin on arsenic-induced liver toxicity in rats. Environ. Toxicol. 30, 628–637. https://doi.org/10.1002/tox.
Pari, L., Amali, D.R., 2005. Protective role of tetrahydrocurcumin (THC) an active principle of turmeric on chloroquine induced hepatotoxicity in rats. J. Pharm. Pharm. Sci. 8, 115–123.
Patra, R.C., Rautray, A.K., Swarup, D., 2011. Oxidative stress in lead and cadmium toxicity and its amelioration. Vet. Med. Int. 2011, 1–9. https://doi.org/10.4061/2011/457327.
Patrick, L., 2006. Lead Toxicity , A Review of the Literature . Part I : Exposure , Evaluation , and Treatment. Altern. Med. Rev. 11.
Rehman, K., Fatima, F., Waheed, I., Akash, M.S.H., 2018. Prevalence of exposure of heavy metals and their impact on health consequences. J. Cell. Biochem. 119, 157–184. https://doi.org/10.1002/jcb.26234.
Saeed, H.S.A., Abdellah, A.M., Abdalla, F.A.B., Abbas, A.R.A., Adam, F.A., Elgazali, N.A., 2017. Biochemical Effects of Lead Toxicity on Serum Total Protein , Albumin and Globulin Levels in Occupationally Exposed Workers in Major Sudanese Cities 7, 132–138.
Sahebkar, A., Serban, M.C., Ursoniu, S., Banach, M., 2015. Effect of curcuminoids on oxidative stress: A systematic review and meta-analysis of randomized

controlled trials. J. Funct. Foods 18, 898–909. https://doi.org/10.1016/j.jff.2015.01.005.
Salahshoor, M., Mohamadian, S., Kakabaraei, S., Roshankhah, S., Jalili, C., 2016. Curcumin improves liver damage in male mice exposed to nicotine. J. Tradit. Complement. Med. 6, 176–183. https://doi.org/10.1016/j.jtcme.2014.11.034.
Salama, S.M., Abdulla, M.A., AlRashdi, A.S., Ismail, S., Alkiyumi, S.S., Golbabapour, S., 2013. Hepatoprotective effect of ethanolic extract of Curcuma longa on thioacetamide induced liver cirrhosis in rats. BMC Complement. Altern. Med. 13, 1472–6882. https://doi.org/10.1186/1472-6882-13-56.
Sarada, S.K.S., Titto, M., Himadri, P., Saumya, S., Vijayalakshmi, V., 2015. Curcumin prophylaxis mitigates the incidence of hypobaric hypoxia-induced altered ion channels expression and impaired tight junction proteins integrity in rat brain. J. Neuroinflammation 12, 1–18. https://doi.org/10.1186/s12974-015-0326-4.
Seddik, L., Bah, T.M., Aoues, A., Brnderdour, M., Silmani, M., 2010. Dried leaf extract protects against lead-induced neurotoxicity in wistar rats. Eur. J. Sci. Res. 42, 139–151.
Shafiu Kamba, A., Ismail, M., Tengku Ibrahim, T.A., Zakaria, Z.A.B., 2013. Synthesis and characterisation of calcium carbonate aragonite nanocrystals from cockle shell powder (Anadara granosa). J. Nanomater. 2013, 9. https://doi.org/10.1155/2013/398357.
Shaikh, J., Ankola, D.D., Beniwal, V., Singh, D., Kumar, M.N.V.R., 2009. Nanoparticle encapsulation improves oral bioavailability of curcumin by at least 9-fold when compared to curcumin administered with piperine as absorption enhancer. Eur. J. Pharm. Sci. 37, 223–230. https://doi.org/10.1016/j.ejps.2009.02.019.
Shalan, M.G., Mostafa, M.S., Hassouna, M.M., El-Nabi, S.E.H., El-Refaie, A., 2005. Amelioration of lead toxicity on rat liver with Vitamin C and silymarin supplements. Toxicology 206, 1–15. https://doi.org/10.1016/j.tox.2004.07.006.
Sharma, A., Sharma, V., Kansal, L., 2009. Amelioration of lead induced hepatotoxicity by Allium sativum. Libyan J. Med. 5, 1–10. https://doi.org/10.4176/091107.
Sidhu, P., Nehru, B., 2004. Lead intoxication: histological and oxidative damage in rat cerebrum and cerebellum. J. Trace Elem. Exp. Med. 17, 45–53. https://doi.org/10.1002/jtra.10052.
Soliman, M.M., Baiomy, A.A., Yassin, M.H., 2015. Molecular and histopathological study on the ameliorative effects of curcumin against lead acetate-induced hepatotoxicity and nephrototoxicity in wistar rats. Biol. Trace Elem. Res. 167, 91–102. https://doi.org/10.1007/s12011-015-0280-0.
Sun, H., Wang, N., Nie, X., Zhao, L., Li, Q., Cang, Z., Chen, C., Lu, M., Cheng, J., Zhai, H., Xia, F., Ye, L., Lu, Y., 2017. Lead exposure induces weight gain in adult rats, accompanied by DNA hypermethylation. PLoS One 12, 1–13. https://doi.org/10.1371/journal.pone.0169958.
Suradkar, S.G., Ghodasara, D.J., Vihol, P., Patel, J., Jaiswal, V., Prajapati, K.S., 2009. Haemato-biochemical alterations induced by lead acetate toxicity in Wistar rats. Vet. World 2, 429–431.
Varnai, V.M., Piasek, M., Blanusša, M., Sarić, M.M., Jureša, D., Kostial, K., 2004. Succimer treatment and calcium supplementation reduce tissue lead in suckling rats. J. Appl. Toxicol. 24, 123–128. https://doi.org/10.1002/jat.961.
Velaga, M.K., Basuri, C.K., Robinson Taylor, K.S., Yallapragada, P.R., Rajanna, S., Rajanna, B., 2014. Ameliorative effects of Bacopa monniera on lead-induced oxidative stress in different regions of rat brain. Drug Chem. Toxicol. 37, 357–364. https://doi.org/10.3109/01480545.2013.866137.
Vlasak, T., Jordakieva, G., Gnambs, T., Augner, C., Crevenna, R., Winker, R., Barth, A., 2019. Science of the total environment blood lead levels and cognitive functioning : a meta-analysis. Sci. Total envi 668, 678–684. https://doi.org/10.1016/j.scitotenv.2019.03.052.
Vorvolakos, T., Arseniou, S., Samakouri, M., 2016. There is no safe threshold for lead exposure: a literature review. Psychiatrike 27, 204–214.
Wang, W., Zhu, R., Xie, Q., Li, A., Xiao, Y., Li, K., Liu, H., Cui, D., Chen, Y., Wang, S., 2012. Enhanced bioavailability and efficiency of curcumin for the treatment of asthma by its formulation in solid lipid nanoparticles. Int. J. Nanomed. 7, 3667–3677. https://doi.org/10.2147/IJN.S30428.
Wani, A.L., Ara, A., Usmani, J.A., 2015. Lead toxicity: A review. Interdiscip. Toxicol. 8, 55–64. https://doi.org/10.1515/intox-2015-0009.
WHO Regional Office for Africa, 2015. Lead Exposure in African Children Contemporary Sources and Concerns.
Yadav, A., Lomash, V., Samim, M., Flora, S.J.S., 2012. Curcumin encapsulated in chitosan nanoparticles: A novel strategy for the treatment of arsenic toxicity. Chem. Biol. Interact. 199, 49–61. https://doi.org/10.1016/j.cbi.2012.05.011.
Yavarpour-bali, H., Ghasemi-kasman, M., Pirzadeh, M., 2019. Curcumin-loaded nanoparticles : a novel therapeutic strategy in treatment of central nervous system disorders 4449–4460.
Yousef, M.I., El-Demerdash, F.M., Radwan, F.M.E., 2008. Sodium arsenite induced biochemical perturbations in rats: Ameliorating effect of curcumin. Food Chem. Toxicol. 46, 3506–3511. https://doi.org/10.1016/j.fct.2008.08.031.
Yu, C.C., Lin, J.L., Lin-Tan, D.T., 2004. Environmental exposure to lead and progression of chronic renal diseases: a four-year prospective longitudinal study. J. Am. Soc. Nephrol. 15, 1016–1022. https://doi.org/10.1097/01.ASN.0000118529.01681.4F.
Yuan, G., Dai, S., Yin, Z., Lu, H., Jia, R., Xu, J., Song, X., Li, L., Shu, Y., Zhao, X., 2014. Toxicological assessment of combined lead and cadmium: Acute and sub-chronic toxicity study in rats. Food Chem. Toxicol. 65, 260–268. https://doi.org/10.1016/j.fct.2013.12.041.
Zhang, Y., Fang, M., Sun, Y., Zhang, T., Shi, N., Li, J., Jin, L., Liu, K., Fu, J., 2018. Curcumin attenuates cerebral ischemia injury in Sprague-Dawley rats and PC12 cells by suppressing overactivated autophagy. J. Photochem. Photobiol. B Biol. 184, 1–6. https://doi.org/10.1016/j.jphotobiol.2018.05.010.